Impact of the quantized transverse motion on radiation emission in a Dirac harmonic oscillator

Tobias N. Wistisen and Antonino Di Piazza
Max-Planck-Institut für Kernphysik, Saupfercheckweg 1, D-69117 Heidelberg, Germany

(Received 15 May 2018; published 24 August 2018)

We investigate the radiation emitted by an ultrarelativistic electron traveling in a one-dimensional parabolic potential. Having in mind a simplified model for beamstrahlung, we consider the realistic case of the electron motion being highly directional, with the transverse momentum being much smaller than the longitudinal one. In this case, we can find approximate solutions of the Dirac equation and we calculate the radiation emission using first-order perturbation theory. We compare our results to those obtained via the semiclassical method of Baier and Katkov, which includes quantum effects due to photon recoil in the radiation emission but ignores the quantum nature of the electron motion. On the one hand, we confirm a prediction of the semiclassical method that the emission spectrum should coincide with that in the case of a linearly polarized monochromatic wave. On the other hand, however, we find that the semiclassical method does not yield the exact result when the quantum number describing the transverse motion becomes small. In this way, we address quantitatively the problem of the limits of validity of the semiclassical method, which is known, generally speaking, to be applicable for large quantum numbers. Finally, we also discuss which beam conditions would be necessary to enter the studied regime where the motion of the particles must also be considered quantum mechanically to yield the correct spectrum.

DOI: 10.1103/PhysRevA.98.022131

I. INTRODUCTION

Strong-field QED is the study of electromagnetic phenomena in the presence of background electromagnetic fields, whose strength approaches a critical limit, called the "Schwinger limit" [1–5]. In this limit, phenomena that are of a purely quantum mechanical nature arise, such as pair production and vacuum birefringence [6–26], and quantum effects in radiation emission become essential [2,13,27–50]. Most of the mentioned studies consider a plane wave as a background field, having in mind processes occurring in the presence of a strong laser field. In this respect, there is also a growing interest in finding out how the basic strong-field QED processes mentioned above are altered in the presence of a laser beam tightly focused in space and not only in time [49,51–56]. In this paper, however, our focus is on a solution to the Dirac equation in a parabolic potential, valid within certain limitations and on different methods of calculating radiation emission; in particular a comparison between a fully quantum calculation, based on the obtained solution to the Dirac equation, compared to a semiclassical method, which can also be used for the case of lasers [8].

The semiclassical operator method developed by Baier and Katkov in 1968 [57] is a powerful method to calculate radiation emission and the probabilities of other quantum processes. Quantum effects such as spin and recoil during emission are included in the method, but the motion of the charged particle is considered as classical, i.e., along a trajectory. Thus, in order to calculate the quantum observables, only the particle's trajectory is needed, which can be found numerically in an arbitrary field configuration. Use of this method to calculate nonlinear Compton scattering in more complex field configurations was the focus of [47]. Now, finding the wave function of an electron in any given field configuration is, in general, an impossible task and it is therefore prudent to ask exactly when the method of Baier and Katkov is applicable. This is, of course, discussed by the authors themselves and the mentioned conditions are that the particle should be ultrarelativistic and that the commutator among the operators corresponding to different velocity components should be negligibly small, in the sense that [27]

$$\frac{|\langle[\hat{\Pi}^{\mu},\hat{\Pi}^{\nu}]\rangle|}{\varepsilon^2}=\frac{|F^{\mu\nu}(x)|}{E_c\gamma^2}\ll 1, \tag{1}$$

where $\hat{\Pi}^{\mu}=\hat{p}^{\mu}+eA^{\mu}(x)$, $\hat{p}^{\mu}$ is the four-momentum operator, $e>0$ is the elementary charge, $A^{\mu}(x)=[\varphi(x),\boldsymbol{A}(x)]$ is the four-vector potential of the external field, $F^{\mu\nu}(x)$ is the electromagnetic field tensor, $E_c=m^2/e$ is the Schwinger critical field, γ is the Lorentz gamma factor, and ε is the particle energy. This means one needs, at least, a field strength of the order of the Schwinger field for this inequality to no longer hold. This condition is, indeed, fulfilled for any currently available electromagnetic field of relevance for the present paper. For the well-known exact solutions of the Dirac equation in the field configurations of a plane wave [2], the semiclassical operator method yields exactly the same result as the full quantum calculation. Therefore, one may ask if there even is a case where the semiclassical operator method would be inadequate. In the final step of the derivation of the method in [27,57], it is stated that since the unfolding of a certain operator has been performed, the expectation value of this operator can be replaced by its corresponding classical value, provided the initial state has large quantum numbers. This is in line with Bohr's correspondence principle. In this paper we find a solution of the Dirac equation in a combined electric and magnetic parabolic potential, assuming only that the typical transverse momentum scale is much smaller than the longitudinal one. In fact, we solve two problems at once since the magnetic component of the field can be turned off,

leaving us with the conventional parabolic electric potential. Using these wave functions, we quantitatively corroborate the statement of Baier and Katkov on the validity of their semiclassical method: For large quantum numbers, we obtain agreement between the two methods, whereas for low quantum numbers, the semiclassical method shows large deviations compared to our calculation. In [58–62] among others, what has been dubbed the "Dirac oscillator" has been studied. All of these studies, however, have in common that they do not introduce the coupling between the charge and the electromagnetic potential A^μ in the usual way by the minimal coupling $p^\mu \to p^\mu + eA^\mu$. The motivation for the alternate coupling in these papers is that it yields an exactly solvable equation which reduces to the quantum harmonic-oscillator problem in the nonrelativistic case. But this is, in fact, not the solution to the problem of a spin-$\frac{1}{2}$ Dirac particle in a parabolic potential in the standard model. The importance of the harmonic-oscillator problem is, in part, that if one Taylor expands any potential around a local minimum, the first term in this expansion will typically be a parabolic term, and so small excitations around the minimum could be explained by applying the model of the harmonic oscillator. In contrast to these papers, we introduce the electromagnetic field by minimal coupling, which yields terms of higher than second order in position, and is thus not exactly solvable. However, we find that under the mentioned circumstance, which is often the case for ultrarelativistic electrons, the terms standing in the way of an analytical solution are small and can be neglected. In [27], the semiclassical method has, naturally, also been employed to study the radiation from the relativistic harmonic oscillator. We included a magnetic field such that the field can also be employed as a simplified model of "beamstrahlung," i.e., the radiation emitted when high-energy dense charged bunches collide. Usually, in future linear colliders, the colliding bunches are of identical shape and oppositely charged, i.e., an electron bunch colliding with a positron bunch. In this case, during the collision, the field from one bunch will alter the shape of the other bunch, and vice versa. The full problem is therefore multiparticle, making it complicated to fully solve it quantum mechanically. However, the classical motion can be solved in this case and therefore the semiclassical method of Baier and Katkov can be applied. To consider when beamstrahlung would become modified due to the quantized transverse motion, we consider a simplified model of beamstrahlung where a single electron interacts with the field of a positron bunch as in this way the positron bunch can be assumed not to change shape during the collision. This solution would still be valid if one studies the collision of a low-density bunch with a high-density bunch, such that the low-density bunch has only a negligible effect on the dense one.

As shown in [27], the result of the semiclassical operator method applied to the one-dimensional oscillator problem yields simply the spectrum obtained in the case of nonlinear Compton scattering in a linearly polarized monochromatic plane wave, as found in, e.g., [2]. However, since this comparison is an important point, below we will also apply the semiclassical operator method to this problem. In Sec. II, we will first consider the electromagnetic field generated from the relativistic positron bunch and indicate how one arrives at the parabolic potential approximation. In Sec. III, we will gain an intuition of the problem and find an approximated analytical solution of the classical equations of motion of the problem, enabling us to apply the semiclassical method of Baier and Katkov in Sec. VI. In Sec. IV, we find the approximate wave functions for the problem at hand and, in Sec. V, we use these wave functions to calculate the transition matrix element of the single-photon radiation emission. In Sec. VII, we do a side-by-side comparison of the power spectra obtained using the two methods of calculation and discuss the different regimes of radiation emission which arise. Finally, in Sec. VIII, we draw the main conclusions of the paper.

We use units where $\hbar = c = 1$, $\alpha = e^2$ and the Feynman slash notation such that $\not{a} = a_\mu \gamma^\mu$, where γ^μ are the Dirac gamma matrices and a^μ is an arbitrary four-vector. We adopt the metric tensor $\eta^{\mu\nu} = \mathrm{diag}(+1, -1, -1, -1)$.

II. MODEL OF THE FIELD

Let us now consider a model of the electromagnetic field from the dense positron bunch. The bunches to be used in linear colliders are ultrarelativistic and usually shaped like sheets, that is, they are much longer than they are wide and much thinner than they are wide. By assuming that the positron bunch propagates along the negative x direction and lies such that the normal vector to this sheet is in the y direction, the rms values of the charge distribution in space are then such that $\Sigma_y \ll \Sigma_z \ll \Sigma_x$ in the laboratory frame. The electron, counterpropagating to the positron bunch, then moves in the positive x direction.

We first consider the field in the comoving frame of the bunch. Here, the transverse beam sizes Σ_y and Σ_z remain unchanged, while the longitudinal becomes longer by a factor of γ_b, which is the Lorentz factor of the bunch, due to the effect of Lorentz contraction. Therefore, in this comoving frame, the bunches are still sheets. The charge density is often modeled as a Gaussian function, that is,

$$\rho'(\boldsymbol{r}') = \frac{Ne}{(2\pi)^{3/2}\Sigma'_x\Sigma'_y\Sigma'_z} e^{-\left(\frac{x'^2}{2\Sigma'^2_x}+\frac{y'^2}{2\Sigma'^2_y}+\frac{z'^2}{2\Sigma'^2_z}\right)}, \tag{2}$$

where primed quantities refer to quantities in the comoving frame and N is the number of positrons in the bunch. In [63], analytical expressions are given for the potential and electric field from such a charge distribution. There, it can be seen, based on the linear expansion around the center of the bunch, that the field gradient in the y direction is greater by a factor of Σ_x/Σ_y than in the x direction. The fact that one component of the field will drive the dynamics can be intuitively understood by thinking of the electric field from a uniformly charged plane. In this case, the electric field is normal to the surface. In our case, when one is close to the center of the bunch, one sees "nearly" such an infinite plane of charge. It is not necessary here to repeat the derivation of [63] and we only mention that the linear expansion of the field component driving the dynamics can be obtained in a quick fashion by using this intuitive picture. In Gauss' law $\boldsymbol{\nabla}' \cdot \boldsymbol{E}'(\boldsymbol{r}') = 4\pi\rho'(\boldsymbol{r}')$, we can then neglect $\partial E'_x/\partial x'$ and $\partial E'_z/\partial z'$ and simply integrate the resulting equation $\partial E'_y/\partial y' = 4\pi\rho'(\boldsymbol{r}')$ with respect to y. This

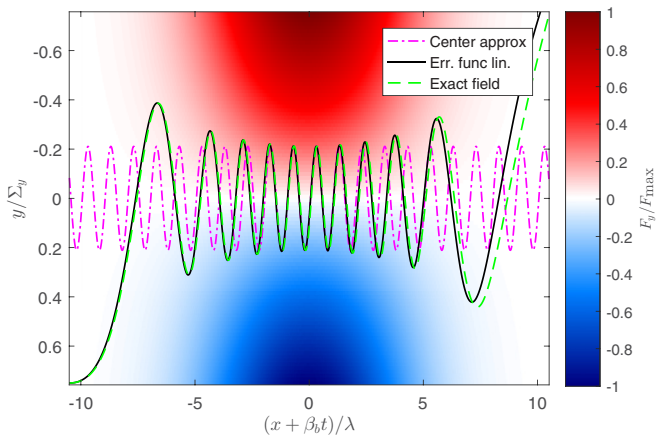

FIG. 1. The y-component F_y of the force exerted by a positron bunch propagating along the negative x direction on an electron propagating in the positive x direction in the x-z plane as a function of position and time. Here, F_{max} is the magnitude of the force at $x+t=0$ and $y/\Sigma_y=0.75$, $\lambda=2\pi/\omega_0$ [see Eq. (25)]. The magenta dash-dotted line corresponds to the approximation valid around the center of the bunch, i.e., the field of Eq. (4). The green dashed line corresponds to the field of Eq. (3), while the continuous black line corresponds to keeping just the first term from the error function in Eq. (3).

results in

$$E'_{y'}(\boldsymbol{r}') = \frac{4\pi Ne}{(2\pi)^{3/2}\Sigma'_x\Sigma'_y\Sigma'_z} \times e^{-\left(\frac{x'^2}{2\Sigma_x'^2}+\frac{z'^2}{2\Sigma_z'^2}\right)}\Sigma'_y\sqrt{\frac{\pi}{2}}\,\mathrm{erf}\left(\frac{y'}{\sqrt{2}\Sigma'_y}\right), \tag{3}$$

where $\mathrm{erf}(x)$ is the error function. Close to the center of the bunch we can keep only the leading-order expansion of the exponential and error function. In this way, we obtain

$$E'_{y'}(\boldsymbol{r}') \simeq \frac{4\pi Ne}{(2\pi)^{3/2}\Sigma'_x\Sigma'_y\Sigma'_z}y'. \tag{4}$$

To obtain the field in the laboratory frame, we perform a Lorentz transformation with velocity given by $-\boldsymbol{\beta}_b$, with $\boldsymbol{\beta}_b$ being the velocity of the bunch. The orthogonal component of the electric field becomes boosted by a factor of the bunch Lorentz factor γ_b, which simplifies with the corresponding change in the bunch length $\Sigma'_z=\gamma_b\Sigma_z$, and one obtains

$$E_y(\boldsymbol{r}) = \frac{4\pi Ne}{(2\pi)^{3/2}\Sigma_x\Sigma_y\Sigma_z}y. \tag{5}$$

A magnetic field arises according to the Lorentz transformation of the electromagnetic fields,

$$\boldsymbol{B}_\perp(\boldsymbol{r}) = -\gamma_b\boldsymbol{\beta}_b\times\boldsymbol{E}'(\boldsymbol{r}') = -\beta_b E_y(\boldsymbol{r})\boldsymbol{e}_3, \tag{6}$$

where $\boldsymbol{e}_3$ is a unit vector in the z direction. In order to neglect the dependence of the fields on x and t, we assume that the dynamics in the y direction occurs on a timescale much shorter than Σ_x. In Fig. 1, we show a comparison of the classical trajectory of the electron through the positron bunch corresponding to the different approximations made for the field from the positron bunch. One can see that even for a quite large initial amplitude of $y/\Sigma_y=0.75$, our approximations result in a trajectory close to the exact one, especially around the center of the bunch. Due to the fact that in a number of situations one can approximate an electromagnetic field as a linear function of a coordinate, this model is still useful not only as a toy model for beamstrahlung, but also to identify the regime where the transverse motion must be treated quantum mechanically, instead of classically. In conclusion, in the remainder of this paper, we will deal with the problem from the laboratory frame and work within the approximation that the only nonzero components of the background electromagnetic field, in the laboratory frame, are given by

$$E_y(\boldsymbol{r}) = \kappa y, \tag{7}$$

$$B_z(\boldsymbol{r}) = -\beta_b\kappa y, \tag{8}$$

where

$$\kappa = \frac{2Ne}{\sqrt{2\pi}\Sigma_x\Sigma_y\Sigma_z} \tag{9}$$

is the field gradient.

III. CLASSICAL MOTION

To gain a basic understanding of the problem at hand, we first consider the classical motion in the given field configuration. We are interested in the case of an ultrarelativistic electron with the motion being mainly directed along the positive x axis, i.e., the x component of the velocity $\boldsymbol{v}$ fulfills the condition $v_x\simeq 1$, whereas the transverse momentum is much smaller than the longitudinal one. In particular, we assume that the initial time is set equal to zero and that $v_z(0)=0$, in such a way that $v_z(t)=0$ for all $t>0$. Since the transverse motion is only along the y direction, it is convenient to introduce the parameter

$$\xi = \gamma_0 v_{y,\max}, \tag{10}$$

where γ_0 is the initial electron Lorentz gamma factor. The parameter ξ then becomes of the order of unity when the transverse motion becomes relativistic. We will restrict ourselves to the (broad) case where $v_{y,\max}\ll 1$ and, therefore, $\xi\ll\gamma_0$. The two conditions $v_x\simeq 1$ and $\xi\ll\gamma_0$ will be employed below to solve the equations of motion. The nonvanishing components of the Lorentz force equation read

$$\frac{dp_x}{dt} = \beta_b e\kappa y v_y, \tag{11}$$

$$\frac{dp_y}{dt} = -e\kappa y - e\beta_b\kappa y v_x = -(1+\beta_b v_x)e\kappa y. \tag{12}$$

Now we use the identity

$$\frac{d\boldsymbol{p}}{dt} = \frac{d\gamma}{dt}m\boldsymbol{v} + \gamma m\frac{d\boldsymbol{v}}{dt}, \tag{13}$$

where m is the electron mass. By using the equation for the variation of the energy

$$m\frac{d\gamma}{dt} = q\boldsymbol{E}\cdot\boldsymbol{v} = -e\kappa y v_y, \tag{14}$$

we obtain

$$\gamma m\frac{dv_x}{dt} = (v_x+\beta_\mathrm{b})e\kappa y v_y, \tag{15}$$

and

$$\gamma m\frac{dv_y}{dt} = -e\kappa y\left(1+\beta_\mathrm{b}v_x - v_y^2\right). \tag{16}$$

Now we write

$$v_x(t) = 1+\delta v_x(t), \tag{17}$$

and

$$\gamma(t) = \gamma_0+\delta\gamma(t), \tag{18}$$

where γ_0 is the initial value of the Lorentz gamma factor for the electron. So we obtain the classical equations of motion in the field of Eqs. (7) and (8) as

$$\frac{d\delta v_x}{dt} = \frac{1}{\gamma_0}\frac{1}{1+\frac{\delta\gamma}{\gamma_0}}(\beta_\mathrm{b}+1+\delta v_x)\frac{e\kappa}{m}yv_y, \tag{19}$$

$$\frac{dv_y}{dt} = -\frac{1}{\gamma_0}\frac{1}{1+\frac{\delta\gamma}{\gamma_0}}\left(1+\beta_\mathrm{b}+\beta_\mathrm{b}\delta v_x - v_y^2\right)\frac{e\kappa}{m}y. \tag{20}$$

Now we wish to find solutions under the conditions $v_y^2(t)\ll 1$, $|\delta v_x(t)|\ll 1$, $|\delta\gamma(t)|\ll\gamma_0$, $1/\gamma_0^2\ll 1$, and $1/\gamma_\mathrm{b}^2\ll 1$. In this case, the equations simplify significantly and we will verify that the obtained solutions verify these conditions. The approximate equations of motion then become

$$\frac{d\delta v_x}{dt} = (1+\beta_\mathrm{b})\frac{e\kappa}{\gamma_0 m}yv_y, \tag{21}$$

$$\frac{dv_y}{dt} = -(1+\beta_\mathrm{b})\frac{e\kappa}{\gamma_0 m}y. \tag{22}$$

Here, one can replace β_b by unity but we prefer to keep the symbol β_b such that we can obtain the case of a harmonic oscillator via the replacement $\beta_\mathrm{b}=0$ because, as seen in Eqs. (7) and (8), only the magnetic field is proportional to β_b. Now the equation for y can be solved with appropriate initial conditions to obtain

$$v_y(t) = \frac{\xi}{\gamma_0}\cos(\omega_0 t), \tag{23}$$

$$y(t) = y_\mathrm{max}\sin(\omega_0 t), \tag{24}$$

where

$$\omega_0 = \sqrt{\frac{(1+\beta_\mathrm{b})e\kappa}{\gamma_0 m}}. \tag{25}$$

And from the definition of Eq. (10), we obtain that the amplitude can be expressed in terms of the previously defined quantities as

$$y_\mathrm{max} = \frac{\xi}{\gamma_0\omega_0}. \tag{26}$$

Now we can solve the equation for the motion along the x direction,

$$\frac{d\delta v_x}{dt} = \omega_0^2 yv_y = \frac{\omega_0}{2}\left(\frac{\xi}{\gamma_0}\right)^2\sin(2\omega_0 t), \tag{27}$$

and, upon integration, we obtain

$$\delta v_x(t) = -\frac{1}{4}\left(\frac{\xi}{\gamma_0}\right)^2\cos(2\omega_0 t)+C_1, \tag{28}$$

where C_1 is a constant of integration. Now, the constant difference between $\delta v_x(t)$ and $v_x(t)$ can be absorbed in the constant of integration C_1 in Eq. (28) such that

$$v_x(t) = -\frac{1}{4}\left(\frac{\xi}{\gamma_0}\right)^2\cos(2\omega_0 t)+C_2. \tag{29}$$

In order to determine the constant C_2, we can use $v_x^2(0)+v_y^2(0) = v_0^2 = 1-1/\gamma_0^2$. Thus, $v_x^2(0) = 1-(1+\xi^2)/\gamma_0^2$ and $v_x(0)\simeq 1-(1+\xi^2)/2\gamma_0^2$, and we can determine the constant of integration C_2 and obtain

$$v_x(t) = 1-\frac{1}{2\gamma_0^2}-\frac{\xi^2}{4\gamma_0^2}-\frac{\xi^2}{4\gamma_0^2}\cos(2\omega_0 t), \tag{30}$$

which, upon integration, yields

$$x(t) = \left(1-\frac{1}{2\gamma_0^2}-\frac{\xi^2}{4\gamma_0^2}\right)t-\frac{\xi^2}{4\gamma_0^2}\frac{\sin(2\omega_0 t)}{2\omega_0}, \tag{31}$$

where we have imposed the condition that $x(0)=0$. Now, it is clear that the conditions for the approximate solutions are fulfilled as long as $\xi\ll\gamma_0$. However we must use Eq. (14) to check when the condition $|\delta\gamma(t)|\ll\gamma_0$ is fulfilled. Using Eq. (14), we obtain

$$\frac{d\gamma}{dt} = -\frac{\omega_0}{1+\beta_\mathrm{b}}\frac{\xi^2}{2\gamma_0}\sin(2\omega_0 t). \tag{32}$$

And so we can integrate to obtain

$$\gamma(t) = \gamma_0+\frac{1}{1+\beta_\mathrm{b}}\frac{\xi^2}{4\gamma_0}[\cos(2\omega_0 t)-1], \tag{33}$$

and therefore

$$\frac{\delta\gamma(t)}{\gamma_0} = \frac{1}{1+\beta_\mathrm{b}}\frac{\xi^2}{4\gamma_0^2}[\cos(2\omega_0 t)-1]. \tag{34}$$

In this way, the condition $|\delta\gamma(t)|\ll\gamma_0$ is equivalent to the condition $\xi\ll\gamma_0$. Therefore, as long as this condition is fulfilled, the neglected terms are smaller than a factor of at least ξ/γ_0 compared to the dominant ones.

IV. SOLUTION OF DIRAC EQUATION

Classically the fields of Eqs. (7) and (8) give a force as in Hooke's law and therefore harmonic oscillations as seen in Sec. III. Harmonic-oscillator wave functions should therefore be involved in the solution of the Dirac equation. We can conveniently choose our electric potential as time independent and so we must find a potential that satisfies $\boldsymbol{E}(\boldsymbol{r}) = -\nabla\varphi(\boldsymbol{r})$. Due to the simple structure of the electric field in Eq. (7), we can choose the potential such that it depends only on the y coordinate, i.e., we have

$$\varphi(y) = -\frac{\kappa y^2}{2}. \tag{35}$$

A vector potential which gives us the magnetic field of Eq. (8) is

$$\boldsymbol{A}(y) = \frac{\beta_b \kappa}{2}(y^2, 0, 0). \tag{36}$$

The Dirac equation in an external field reads

$$[\hat{\not{p}} + e\not{A}(\boldsymbol{r}) - m]\psi(\boldsymbol{r}, t) = 0, \tag{37}$$

where $\psi(\boldsymbol{r}, t)$ is the electron bispinor wave function. This can also be rewritten as

$$i\frac{\partial \psi(\boldsymbol{r}, t)}{\partial t} = \hat{H}\psi(\boldsymbol{r}, t), \tag{38}$$

with

$$\hat{H} = \boldsymbol{\alpha} \cdot \hat{\boldsymbol{\Pi}} - e\varphi(\boldsymbol{r}) + \gamma^0 m, \tag{39}$$

where $\boldsymbol{\alpha}^i = \gamma^0\gamma^i$, $i = 1, 2, 3$, and $\boldsymbol{\Pi}_i = \hat{\boldsymbol{p}}_i + e\boldsymbol{A}_i(\boldsymbol{r})$ (for electron). We consider a problem where the potentials have no time dependence and then take the usual approach [64,65] of finding the stationary states, and write

$$\psi(\boldsymbol{r}, t) = e^{-i\varepsilon t}\begin{pmatrix}\phi(\boldsymbol{r})\\ \chi(\boldsymbol{r})\end{pmatrix}, \tag{40}$$

where ε will be the energy. This leads to

$$[\varepsilon + e\varphi(\vec{r}) - m]\phi(\boldsymbol{r}) = \boldsymbol{\sigma} \cdot [-i\boldsymbol{\nabla} + e\boldsymbol{A}(\boldsymbol{r})]\chi(\boldsymbol{r}), \tag{41}$$

$$[\varepsilon + e\varphi(\vec{r}) + m]\chi(\boldsymbol{r}) = \boldsymbol{\sigma} \cdot [-i\boldsymbol{\nabla} + e\boldsymbol{A}(\boldsymbol{r})]\phi(\boldsymbol{r}), \tag{42}$$

where we have used that $\boldsymbol{\alpha}^i = \left(\begin{smallmatrix}0 & \sigma^i\\ \sigma^i & 0\end{smallmatrix}\right)$, where $\boldsymbol{\sigma}^i$ denote the three Pauli matrices. Now, from Eq. (42), we find

$$\chi(\boldsymbol{r}) = \frac{1}{\varepsilon + e\varphi(y) + m}\boldsymbol{\sigma} \cdot \hat{\boldsymbol{\Pi}}\phi(\boldsymbol{r}), \tag{43}$$

and inserting this in Eq. (41), we obtain a differential equation for $\phi(\boldsymbol{r})$,

$$\begin{aligned}&[\varepsilon + e\varphi(y) - m]\phi(\boldsymbol{r})\\ &\quad = \boldsymbol{\sigma} \cdot [-i\boldsymbol{\nabla} + e\boldsymbol{A}(y)]\frac{1}{\varepsilon + e\varphi(y) + m}\boldsymbol{\sigma} \cdot \hat{\boldsymbol{\Pi}}\phi(\boldsymbol{r}).\end{aligned} \tag{44}$$

To find the solution for $\phi(\boldsymbol{r})$, we need to rewrite this such that we can isolate the Laplacian of $\phi(\boldsymbol{r})$. The product rule for the gradient gives us a term where it acts on $[\varepsilon + e\varphi(y) + m]^{-1}$ and one where it acts on $\boldsymbol{\sigma} \cdot \hat{\boldsymbol{\Pi}}\phi(\boldsymbol{r})$, which gives us

$$\begin{aligned}&[\varepsilon + e\varphi(y) - m]\phi(\boldsymbol{r})\\ &\quad = i\boldsymbol{\sigma}_y \cdot \frac{e\varphi'(y)}{[\varepsilon + e\varphi(y) + m]^2}\boldsymbol{\sigma} \cdot \hat{\boldsymbol{\Pi}}\phi(\boldsymbol{r})\\ &\qquad + \frac{1}{\varepsilon + e\varphi(y) + m}[\boldsymbol{\sigma} \cdot \hat{\boldsymbol{\Pi}}]^2\phi(\boldsymbol{r}).\end{aligned} \tag{45}$$

Multiplying by $[\varepsilon + e\varphi(y) + m]$ on both sides, we obtain

$$\begin{aligned}&\{[\varepsilon + e\varphi(y)]^2 - m^2\}\phi(\boldsymbol{r})\\ &\quad = i\boldsymbol{\sigma}_y \cdot \frac{1}{\varepsilon + e\varphi(y) + m}e\varphi'(y)\boldsymbol{\sigma} \cdot \hat{\boldsymbol{\Pi}}\phi(\boldsymbol{r}) + [\boldsymbol{\sigma} \cdot \hat{\boldsymbol{\Pi}}]^2\phi(\boldsymbol{r})\\ &\quad = -i\frac{1}{\varepsilon + e\varphi(y) + m}[\boldsymbol{\sigma}_y \cdot eE_y(y)]\boldsymbol{\sigma} \cdot \hat{\boldsymbol{\Pi}}\phi(\boldsymbol{r})\\ &\qquad + [\boldsymbol{\sigma} \cdot \hat{\boldsymbol{\Pi}}]^2\phi(\boldsymbol{r})\\ &\quad = \frac{-i}{\varepsilon + e\varphi(y) + m}\{eE_y(y)\hat{\boldsymbol{\Pi}}_y + i\boldsymbol{\sigma} \cdot [e\boldsymbol{E}(y) \times \hat{\boldsymbol{\Pi}}]\}\phi(\boldsymbol{r})\\ &\qquad + [\boldsymbol{\sigma} \cdot \hat{\boldsymbol{\Pi}}]^2\phi(\boldsymbol{r}).\end{aligned} \tag{46}$$

Now we need to consider the term $[\boldsymbol{\sigma} \cdot \hat{\boldsymbol{\Pi}}]^2$ by letting it act on a test function f,

$$\begin{aligned}&\{\boldsymbol{\sigma} \cdot [\hat{\boldsymbol{p}} + e\boldsymbol{A}(y)]\}\{\boldsymbol{\sigma} \cdot [\hat{\boldsymbol{p}}f + e\boldsymbol{A}(y)f]\}\\ &\quad = \hat{\boldsymbol{p}}^2 f + \boldsymbol{\sigma} \cdot \{\boldsymbol{\nabla} \times [e\boldsymbol{A}(y)]\}f\\ &\qquad + 2eA_x(y)\hat{p}_x f + e^2A^2(y)f.\end{aligned} \tag{47}$$

Then, finally, we obtain

$$\begin{aligned}&[\hat{\boldsymbol{p}}^2 + e\boldsymbol{\sigma} \cdot \boldsymbol{B}(y) + 2eA_x(y)\hat{p}_x\\ &\quad - 2\varepsilon e\varphi(y) + e^2A^2(y) - e^2\varphi^2(y)\\ &\quad - i\frac{1}{\varepsilon + e\varphi(y) + m}\{eE_y\hat{\Pi}_y + i\boldsymbol{\sigma} \cdot [e\boldsymbol{E}(y) \times \hat{\boldsymbol{\Pi}}]\}\\ &\quad - (\varepsilon^2 - m^2)]\phi(\boldsymbol{r}) = 0.\end{aligned} \tag{48}$$

This is the exact differential equation for $\phi(\boldsymbol{r})$. If one divides this equation with 2ε, it is seen that we obtain an equation of the form $[\hat{\boldsymbol{p}}^2/2\varepsilon - e\varphi(y) + eA_x(y)\hat{p}_x/\varepsilon + \cdots]\phi(\boldsymbol{r}) = 0$, which looks like the usual Schrödinger equation for the nonrelativistic harmonic oscillator with potential energy $V(y) = -e\varphi(y)$, except with the "relativistic mass" ε and an additional term of the same size from the magnetic field. Therefore, we will posit that in Eq. (48), the dominant terms driving the dynamics are the terms $2eA_x(y)\hat{p}_x - 2\varepsilon e\varphi(y)$, and we compare the sizes of the additional terms to these. We will try with a separable solution which yields free motion in the x direction such that this becomes $2eA_x(y)p_x$ (no longer an operator).

A. $e^2\varphi^2(y)$ term

If $e^2\varphi^2(y)$ should be much smaller than $-2\varepsilon e\varphi(y)$, we should have that $2\varepsilon \gg -e\varphi(y)$. The most stringent condition is then to use $-e\varphi_{\max} = -e\varphi(y_{\max}) = e\kappa y_{\max}^2/2 = e\kappa\xi^2/2\gamma_0^2\omega_0^2$. Our condition then becomes $1 \gg \frac{\xi^2}{\gamma_0^2}\frac{1}{4(1+\beta_b)}$, a condition which will be fulfilled as we require exactly that $\xi \ll \gamma_0$. The same argument goes for the $e^2A^2(y)$ term.

B. $e\boldsymbol{\sigma} \cdot \boldsymbol{B}(y)$ term

Here we should have $-2\varepsilon e\varphi(y) \gg eB_z(y)$ corresponding to

$$2\varepsilon\frac{e\kappa y^2}{2} \gg e\kappa y, \tag{49}$$

which reduces to

$$y \gg \frac{1}{\varepsilon}. \tag{50}$$

We are looking for the solutions of the quantum problem analogous to the classical solutions, and therefore we still have $\varepsilon \simeq \gamma_0 m$; therefore, $1/\varepsilon$ is roughly the Compton wavelength divided by a factor of γ_0. The problem could, in fact, be solved while including this term, and the effect would be that the spin-up and spin-down wave functions are shifted by the distance $1/\varepsilon$ compared to each other. This is, however, completely negligible. As we will see later, the transition to the

new regime happens when the typical length of the problem becomes of the order of the Compton wavelength, and this condition differs by a factor of $1/\gamma_0$ compared to this.

C. $\frac{eE_y\hat{\Pi}_y}{\varepsilon+e\varphi(y)+m}$ term

We obtain the most stringent condition by inserting the maximum value of the classical momentum and so

$$\frac{eE_y\hat{\Pi}_y}{\varepsilon+e\varphi(y)+m}\simeq\frac{e\kappa y p_{y,\max}}{\varepsilon}\simeq\frac{e\kappa y m\xi}{\varepsilon}. \tag{51}$$

We should then have

$$\frac{e\kappa y m\xi}{\varepsilon}\ll -2\varepsilon e\varphi(y)=\varepsilon e\kappa y^2, \tag{52}$$

which reduces to

$$y\gg\frac{\xi}{\gamma_0}\frac{1}{\varepsilon}, \tag{53}$$

and since we require that $\gamma_0\gg\xi$ if Eq. (50) is fulfilled, then so is Eq. (53).

D. $\frac{\boldsymbol{\sigma}\cdot(e\boldsymbol{E}\times\hat{\boldsymbol{\Pi}})}{\varepsilon+e\varphi(y)+m}$ term

We have $\boldsymbol{\sigma}\cdot(\boldsymbol{E}\times\hat{\boldsymbol{\Pi}})=\boldsymbol{\sigma}_x E_y(y)p_z-\boldsymbol{\sigma}_z E_y(y)[p_x+eA_x(y)]$. The previous terms have either had the matrix structure of the identity or $\boldsymbol{\sigma}_z$, while here we also have a term proportional to $\boldsymbol{\sigma}_x$, i.e., a mixing between the spin states. The $\boldsymbol{\sigma}_z$ term is of the same size as the one from Sec. IV B and therefore is negligible. The mixing term will be even smaller, as p_z will be zero initially and of the order of m in the final state, so a factor of γ_0 smaller than the already negligible small correction.

Now that we have argued for the smallness of the additional terms, we are left with the equation

$$[-\boldsymbol{\nabla}^2+e\kappa\beta y^2(-i\partial_x)+\varepsilon e\kappa y^2-(\varepsilon^2-m^2)]\phi(\boldsymbol{r})=0. \tag{54}$$

To solve this equation, we try the ansatz $\phi(\boldsymbol{r})=I(y)e^{ip_x x+ip_z z}\boldsymbol{s}$, where $\boldsymbol{s}$ is any two-component vector and so we obtain the following differential equation:

$$\left[\frac{d^2}{d\eta^2}-\eta^2+a\right]I(\eta)=0, \tag{55}$$

where we have defined

$$a=L^2\left(\varepsilon^2-p_x^2-p_z^2-m^2\right), \tag{56}$$

and

$$\frac{1}{L}=\sqrt[4]{e\kappa(\beta_{\mathrm{b}}p_x+\varepsilon)}, \tag{57}$$

and the dimensionless variable is defined by $\eta=y/L$.

This has normalizable solutions when $a=2n+1$ with n integer (see, e.g., [66,67]), which we denote $I_n(\eta)$. And so the solutions to Eq. (54) are given by

$$\phi_n(\boldsymbol{r})=e^{i(p_x x+p_z z)}I_n(\eta(y))\boldsymbol{s}. \tag{58}$$

Because the solutions are quantized with quantum number n, we identify $\varepsilon^2\to\varepsilon_n^2$ and must have that the constants are related by

$$\varepsilon_n^2=\frac{1}{L^2}(2n+1)+p_x^2+p_z^2+m^2, \tag{59}$$

and the solutions to Eq. (55) can be written explicitly as

$$I_n(\eta)=N_n e^{-\eta^2/2}H_n(\eta), \tag{60}$$

where N_n is a normalization constant to be found and $H_n(\eta)$ are the Hermite polynomials normalized such that $\int_{-\infty}^{\infty}H_m(x)H_n(x)e^{-x^2}dx=\sqrt{\pi}2^n n!\delta_{nm}$, where δ_{nm} is the Kronecker delta function. In this problem, we deal with a bound motion in the y direction and, therefore, we would expect the wave functions to be somewhat bounded within a certain region. Indeed, it is the case that the functions $I_n(\eta)$ will rapidly decay to zero when $\eta>\sqrt{2n}$ and very sharply for $n\gg 1$. Therefore, we can relate the classical amplitude of the motion by $y_{\max}=L\sqrt{2n}$. In Eq. (59), we see that $(2n+1)/L^2$ seemingly takes on the role as the squared momentum in the y direction. Replacing $2n$ with $y_{\max}$, according to this relation, one obtains approximately that $2n/L^2\to\xi^2m^2$ such that we have $|p_y|\simeq\xi m$, which is the expected size from the study of the classical dynamics. Our regime of validity, $\xi/\gamma_0\ll 1$, can then also be translated to a condition on n that $2n/L^2\ll\varepsilon^2$. We would like to normalize $I_n(\eta)$ such that

$$\int|I_n(\eta)|^2dy=1, \tag{61}$$

which gives us

$$N_n=\frac{1}{\sqrt{2^n L\sqrt{\pi}n!}}. \tag{62}$$

So we have our solutions to the Dirac equation as

$$\psi(\boldsymbol{r},t)=\frac{1}{\sqrt{2L_xL_z}}\begin{pmatrix}I_n(\eta)\boldsymbol{s}\\ \frac{\boldsymbol{\sigma}\cdot[-i\boldsymbol{\nabla}+e\boldsymbol{A}(y)]}{\varepsilon+e\varphi(y)+m}I_n(\eta)\boldsymbol{s}\end{pmatrix}e^{i(p_x x+p_z z-\varepsilon_n t)}, \tag{63}$$

where L_xL_z is a normalization area in the xz plane (one particle per area). When calculating the transition rate, we will need to sum over two linearly independent spin states which we choose by setting $\boldsymbol{s}=(1,0)$ corresponding to what we will call spin up ($\uparrow$) and $\boldsymbol{s}=(0,1)$ to spin down ($\downarrow$). In this way, we can write

$$\psi_\uparrow(\boldsymbol{r},t)=\frac{1}{\sqrt{2L_xL_z}}e^{i(p_x x+p_z z-\varepsilon_n t)}U_\uparrow(y), \tag{64}$$

$$\psi_\downarrow(\boldsymbol{r},t)=\frac{1}{\sqrt{2L_xL_z}}e^{i(p_x x+p_z z-\varepsilon_n t)}U_\downarrow(y), \tag{65}$$

where

$$U_\uparrow(y)=\begin{pmatrix}I_n(\eta)\\ 0\\ \frac{p_z I_n(\eta)}{\varepsilon_n+e\varphi(y)+m}\\ \frac{p_x I_n(\eta)+I_n(\eta)\eta^2 C+\frac{1}{L}\frac{dI_n(\eta)}{d\eta}}{\varepsilon_n+e\varphi(y)+m}\end{pmatrix}, \tag{66}$$

$$U_\downarrow(y)=\begin{pmatrix}0\\ I_n(\eta)\\ \frac{p_x I_n(\eta)+I_n(\eta)\eta^2 C-\frac{1}{L}\frac{dI_n(\eta)}{d\eta}}{\varepsilon_n+e\varphi(y)+m}\\ \frac{-p_z I_n(\eta)}{\varepsilon_n+e\varphi(y)+m}\end{pmatrix}. \tag{67}$$

Here we obtained a more explicit form than in Eq. (63) by inserting the Pauli matrices, i.e.,

$$\begin{aligned}\boldsymbol{\sigma}\cdot\left[-i\boldsymbol{e}_2\frac{d}{dy}+e\boldsymbol{A}(y)\right]I_n(\eta)&\\ =y^2I_n(\eta)\frac{e\kappa\beta_\mathrm{b}}{2}\boldsymbol{\sigma}_x-i\boldsymbol{\sigma}_y\frac{dI_n(\eta)}{dy}&\\ =\begin{pmatrix}0 & I_n(\eta)\eta^2C-\frac{1}{L}\frac{dI_n}{d\eta}\\ I_n(\eta)\eta^2C+\frac{1}{L}\frac{dI_n}{d\eta} & 0\end{pmatrix},&\quad(68)\end{aligned}$$

where $\boldsymbol{e}_2$ is a unit vector in the y direction and we defined $C=\frac{e\kappa\beta_\mathrm{b}L^2}{2}$.

Finally, since the potential $[-e\varphi(y)]$ in the denominator is much smaller than the energy ε_n (this is the same condition as in Sec. IV A), we can make the following approximation, valid when $\gamma_0\gg\xi$:

$$\begin{aligned}&\frac{p_xI_n(\eta)+I_n\eta^2C+\frac{1}{L}\frac{dI_n(\eta)}{d\eta}}{\varepsilon_n+e\varphi(y)+m}\\ &=\frac{p_xI_n(\eta)+I_n(\eta)\eta^2C+\frac{1}{L}\frac{dI_n(\eta)}{d\eta}}{(\varepsilon_n+m)\left[1+\frac{e\varphi(y)}{\varepsilon_n+m}\right]}\\ &\simeq\frac{p_xI_n(\eta)+I_n(\eta)\eta^2C+\frac{1}{L}\frac{dI_n(\eta)}{d\eta}}{(\varepsilon_n+m)}\left[1-\frac{e\varphi(y)}{\varepsilon_n+m}\right].\end{aligned}\quad(69)$$

In this product, we do not need to keep all terms, as some are completely negligible. We only want to keep what corresponds to the leading order in ξ/γ_0. Considering first the term proportional to $I_n(\eta)$, we must consider $[p_xI_n(\eta)+I_n(\eta)\eta^2C][1-\frac{e\varphi(y)}{\varepsilon_n+m}]$. First we must realize that the first term in the first brackets, being proportional to p_x, is much larger than the other term in these brackets. This can be seen by considering that

$$\eta^2C\lesssim\frac{y_\mathrm{max}^2}{L^2}\frac{e\kappa\beta_\mathrm{b}L^2}{2}=\left(\frac{\xi}{\gamma_0}\right)^2\frac{\beta_\mathrm{b}}{2}\frac{\gamma_0m}{(1+\beta_\mathrm{b})},\quad(70)$$

and therefore the second term in the numerator is of the order of ξ^2/γ_0^2 compared to the first. Therefore, we have

$$\begin{aligned}&[p_xI_n(\eta)+I_n(\eta)\eta^2C]\left[1-\frac{e\varphi(y)}{\varepsilon_n+m}\right]\\ &\simeq p_xI_n(\eta)+I_n(\eta)\eta^2C-\frac{e\varphi(y)}{\varepsilon_n+m}p_xI_n(\eta)\\ &=p_xI_n(\eta)+I_n(\eta)\eta^2D,\end{aligned}\quad(71)$$

where $D=\frac{e\kappa(\frac{p_x}{\varepsilon_n+m}+\beta_\mathrm{b})L^2}{2}$. From the first to second line, we could neglect the product of the two small quantities as they would be higher than the leading order in ξ/γ_0. Similarly, we can approximate $D\simeq\frac{e\kappa(1+\beta_\mathrm{b})L^2}{2}$, as the error in doing this leads only to a term of higher than leading order in ξ/γ_0. For the term proportional to $dI_n/d\eta$, we can simply approximate

$$\frac{1}{L}\frac{dI_n(\eta)}{d\eta}\left[1-\frac{e\varphi(y)}{\varepsilon_n+m}\right]\simeq\frac{1}{L}\frac{dI_n(\eta)}{d\eta}.\quad(72)$$

This is due to the fact that $1/LdI_n(\eta)/d\eta$ came from the momentum operator in the y direction applied to $I_n(\eta)$ and therefore this is already proportional to ξ/γ_0, and including the product with the other small quantity would lead to terms of the order of ξ^3/γ_0^3 and is therefore smaller than the leading order. We have confirmed with our numerical examples of calculation, shown later, that keeping the terms neglected here makes no difference. As such, we finally obtain

$$U_\uparrow(y)=\begin{pmatrix}I_n(\eta)\\ 0\\ \frac{p_zI_n(\eta)}{\varepsilon_n+m}\\ \frac{p_xI_n(\eta)+I_n(\eta)\eta^2D+\frac{1}{L}\frac{dI_n(\eta)}{d\eta}}{\varepsilon_n+m}\end{pmatrix},\quad(73)$$

$$U_\downarrow(y)=\begin{pmatrix}0\\ I_n(\eta)\\ \frac{p_xI_n(\eta)+I_n(\eta)\eta^2D-\frac{1}{L}\frac{dI_n(\eta)}{d\eta}}{\varepsilon_n+m}\\ \frac{-p_zI_n(\eta)}{\varepsilon_n+m}\end{pmatrix}.\quad(74)$$

It was earlier stated that the normalization was for one particle per area, however unproven. To show that this is correct within our approximation, we calculate $\int\psi^\dagger(\boldsymbol{r},t)\psi(\boldsymbol{r},t)dV$. We have

$$\begin{aligned}&\int\psi_\uparrow^\dagger(\boldsymbol{r},t)\psi_\uparrow(\boldsymbol{r},t)dV\\ &=\frac{1}{2}\int dy\Big\{|I_n(\eta)|^2\\ &\quad+\left[\frac{p_xI_n(\eta)+I_n(\eta)\eta^2C+\frac{1}{L}\frac{dI_n(\eta)}{d\eta}}{\varepsilon_n+e\varphi(y)+m}\right]^2\Big\},\end{aligned}\quad(75)$$

where the integration over $dxdz$ has canceled out with the area L_xL_z in the front factor of Eq. (64). We show here the case of spin up, but the result is the same for spin down.

By using the properties that the derivative of the $I_n(\eta)$ function, as they are harmonic-oscillator wave functions, is related to the stepped up and down wave functions, we find that a factor of

$$\frac{1}{\sqrt{1+\frac{p_x^2-(E_n+m)^2+\left(\frac{3}{2}n^2+\frac{3}{2}n+\frac{3}{4}\right)D^2+\left(\frac{1}{L^2}+p_xD\right)\left(n+\frac{1}{2}\right)}{2(\varepsilon_n+m)^2}}}\quad(76)$$

is to be multiplied onto the wave function to ensure exact normalization. To estimate the size of this correction, we also need to know the typical size of n. As mentioned earlier, the solutions $I_n(\eta)$ rapidly drop off, for large n, when $\eta^2>2n$. We have that $e[A_x(y)-\varphi(y)]\sim D\eta^2$ and, therefore, $nD\sim-e\varphi(y_\mathrm{max})$. Thus we have terms that are of the order of $-e\varphi(y_\mathrm{max})/\varepsilon_n$ or this factor squared, which is therefore of the same size as the correction found in Sec. IV A. The term n/L^2 can be seen to be of the same order by replacing $n\sim-e\varphi(y_\mathrm{max})/D$ and using the definition of L. Therefore, as long as $\gamma_0\gg\xi$, the normalization of Eqs. (64) and (65) is correct within our accuracy.

V. RADIATION EMISSION

Now that we have obtained the wave functions, we can calculate the probability of radiation emission by using the transition matrix element from an initial state $\psi_i(x)$ to a final state $\psi_f(x)$ while emitting a photon with momentum

four-vector $k^\mu = (\omega, \boldsymbol{k})$ and polarization ϵ, which is given by

$$S_{fi} = \int d^4x \bar{\psi}_f(x) i e \sqrt{\frac{4\pi}{2\omega V}} \not{\epsilon}^* e^{ikx} \psi_i(x). \tag{77}$$

Then the differential rate of emission dW is usually given by

$$dW = |S_{fi}|^2 \frac{1}{T} \frac{V d^3 p_f}{(2\pi)^3} \frac{V d^3 k}{(2\pi)^3}, \tag{78}$$

where V is the normalization volume and T is the interaction time, factors which eventually cancel out. In our case, the density of the final states of the electron instead becomes $\frac{V d^3 p_f}{(2\pi)^3} \to \frac{dp_x dp_z L_x L_z}{(2\pi)^2} \sum_{n_f}$, where $L_x L_z$ is a normalization area. This change is due simply to the fact that one quantum number is discrete instead of continuous. Inserting our wave functions from Eq. (65), we obtain

$$\begin{aligned} S_{fi} = & i e \sqrt{\frac{4\pi}{2\omega V}} \frac{1}{2 L_x L_z} \int d^4x \bar{U}_f(y) \not{\epsilon}^* U_i(y) \\ & \times e^{-i k_y y} e^{i(p_{x,i} - p_{x,f} - k_x)x} e^{i(p_{z,i} - p_{z,f} - k_z)z} \\ & \times e^{i(\varepsilon_f + \omega - \varepsilon_i)t}, \end{aligned} \tag{79}$$

and carrying out the trivial integrations, we obtain

$$\begin{aligned} S_{fi} = & i e \sqrt{\frac{4\pi}{2\omega V}} \frac{1}{2 L_x L_z} (2\pi)^3 \int \bar{U}_f(y) \not{\epsilon}^* U_i(y) e^{-i k_y y} dy \\ & \times \delta(p_{x,i} - p_{x,f} - k_x) \delta(p_{z,i} - p_{z,f} - k_z) \\ & \times \delta(\varepsilon_f + \omega - \varepsilon_i). \end{aligned} \tag{80}$$

Since we need this quantity squared, we must consider the meaning of the δ function squared. Here we take the usual approach to obtain factors of the normalization volume and time, i.e., $[\delta(p_{x,i} - p_{x,f} - k_x)\delta(p_{z,i} - p_{z,f} - k_z)\delta(\varepsilon_f + \omega - \varepsilon_i)]^2 = \frac{L_x L_z T}{(2\pi)^3} \delta(p_{x,i} - p_{x,f} - k_x)\delta(p_{z,i} - p_{z,f} - k_z)\delta(\varepsilon_f + \omega - \varepsilon_i)$, and so we obtain

$$\begin{aligned} |S_{fi}|^2 = & \frac{4\pi e^2}{2\omega V} \frac{1}{(2 L_x L_z)^2} (2\pi)^6 \\ & \times \left| \int \bar{U}_f(y) \not{\epsilon}^* U_i(y) e^{-i k_y y} dy \right|^2 \\ & \times \frac{L_x L_z T}{(2\pi)^3} \delta(p_{x,i} - p_{x,f} - k_x) \delta(p_{z,i} - p_{z,f} - k_z) \\ & \times \delta(\varepsilon_f + \omega - \varepsilon_i). \end{aligned} \tag{81}$$

Now integrating over final electron momentum, we obtain

$$\begin{aligned} & \int \frac{dp_x dp_z L_x L_z}{(2\pi)^2} \sum_{n_f} |S_{fi}|^2 \\ & = \sum_{n_f} \frac{e^2}{4\omega V} (2\pi)^2 \left| \int \bar{U}_f(y) \not{\epsilon}^* U_i(y) e^{-i k_y y} dy \right|^2 \\ & \quad \times T \delta(\varepsilon_f + \omega - \varepsilon_i). \end{aligned} \tag{82}$$

Now we must only account for the photon density of states from Eq. (78) and we obtain the differential rate as

$$\begin{aligned} dW = & \sum_{n_f} \frac{e^2}{8\pi\omega} \left| \int \bar{U}_f(y) \not{\epsilon}^* U_i(y) e^{-i k_y y} dy \right|^2 \\ & \times \delta(\varepsilon_f + \omega - \varepsilon_i) \omega^2 d\omega d\Omega. \end{aligned} \tag{83}$$

Now we wish to integrate over $d\cos\theta$ in $d\Omega = d\Phi d\cos\theta$ to get rid of the last δ function. To do this, we use the energy relation of Eq. (59) to write the final energy and use that the momentum δ functions have fixed $p_{x,f} = p_{x,i} - k_x$ and $p_{z,f} = p_{z,i} - k_z$. Now writing the photon momentum vector $\boldsymbol{k}$ in spherical coordinates,

$$\boldsymbol{k} = \omega(\cos\theta, \sin\theta\cos\Phi, \sin\theta\sin\Phi), \tag{84}$$

we have

$$p_{z,f} = -k_z = -\omega\sin\theta\sin\Phi, \tag{85}$$

$$p_{x,f} = p_{x,i} - \omega\cos\theta. \tag{86}$$

In this case, Eq. (59) for the final energy ε_f becomes

$$\begin{aligned} \varepsilon_f^2 = & (2n+1)\sqrt{e\kappa[p_{x,i} + \varepsilon_i - \omega(1+\cos\theta)]} \\ & + (p_{x,i} - \omega\cos\theta)^2 + \omega^2\sin^2\theta\sin^2\Phi + m^2. \end{aligned} \tag{87}$$

Now we wish to carry out the integration over $d\cos\theta$ so we must transform the δ function so

$$\delta(\varepsilon_f(\cos\theta) + \omega - \varepsilon_i) = \frac{\delta(\cos\theta - \cos\theta_0)}{\left| \frac{d\varepsilon_f}{d\cos\theta}(\cos\theta) \right|}, \tag{88}$$

where $\cos\theta_0$ is the solution to the equation

$$\varepsilon_f(\cos\theta) + \omega - \varepsilon_i = 0, \tag{89}$$

which we will find later. We obtain, from Eq. (87),

$$\begin{aligned} \frac{d\varepsilon_f}{d\cos\theta} = & \frac{1}{\varepsilon_f} \Bigg[-(2n+1) \frac{e\kappa\omega}{4\sqrt{e\kappa[p_{x,i} + \varepsilon_i - \omega(1+\cos\theta)]}} \\ & - \omega p_{x,i} + \omega^2 \cos\theta \cos^2\Phi \Bigg]. \end{aligned} \tag{90}$$

And so we have integrated over all the δ functions and can write the differential rate as

$$\begin{aligned} dW = & \sum_{n_f} \frac{e^2}{8\pi\omega'} \left| \int \bar{U}_f(y) \not{\epsilon}^* U_i(y) e^{-i k_y y} dy \right|^2 \\ & \times \frac{1}{\left| \frac{d\varepsilon_f}{d\cos\theta}(\theta_0) \right|} \omega^2 d\omega d\Phi. \end{aligned} \tag{91}$$

To find the solution of Eq. (89) we will recall that we consider ultrarelativistic particles such that θ is small, meaning we can perform the series expansions of $\cos\theta \simeq 1 - \frac{\theta^2}{2}$ and $\sin\theta \simeq \theta$.

Inserting this in Eq. (87), we obtain

$$\theta_0 = [(\varepsilon_i-\omega)^2-(2n+1)\sqrt{e\kappa(p_{x,i}+\varepsilon_i-2\omega)} -(p_{x,i}-\omega)^2-m^2]^{1/2}/[(p_{x,i}-\omega)\omega+\omega^2\sin^2\Phi +\frac{\omega/4}{p_{x,i}+\varepsilon_i-2\omega}(2n+1)\sqrt{e\kappa(p_{x,i}+\varepsilon_i-2\omega)}]^{1/2}. \tag{92}$$

Now we have all the quantities necessary to evaluate the rate from Eq. (91).

VI. BAIER METHOD

From [47,68], it can be seen that the differential power emitted in the semiclassical operator method is given by

$$\frac{d^2P}{d\omega d\Omega}=\frac{1}{T}\frac{e^2}{4\pi^2}\omega'^2\left(\frac{\varepsilon^2+\varepsilon'^2}{2\varepsilon^2}\left|\int_{-\infty}^{\infty}(\boldsymbol{n}-\boldsymbol{v})e^{i\omega'(t-\boldsymbol{n}\cdot\boldsymbol{r})}dt\right|^2 +\frac{\omega^2m^2}{2\varepsilon^4}\left|\int_{-\infty}^{\infty}e^{i\omega'(t-\boldsymbol{n}\cdot\boldsymbol{r})}dt\right|^2\right), \tag{93}$$

where $\varepsilon'=\varepsilon-\omega$, $\omega'=\omega\varepsilon/(\varepsilon-\omega)$, $\boldsymbol{n}=(\cos\theta, \sin\theta\cos\Phi, \sin\theta\sin\Phi)$ is the direction of emission. Therefore, Eq. (93) allows for the determination of the differential power emitted, including quantum effects, for a given classical trajectory described by $\boldsymbol{r}(t)$ and $\boldsymbol{v}(t)$, which are the classical position and velocity vectors, respectively. It is beneficial to first look at the integral from the second term and insert the motion found in Sec. III,

$$\int_{-\infty}^{\infty}e^{i\omega'(t-\boldsymbol{n}\cdot\boldsymbol{r})}dt =\int_{-\infty}^{\infty}e^{i\omega'\left\{t-\cos\theta\left[\left(1-\frac{1}{2\gamma_0^2}-\frac{\xi^2}{4\gamma_0^2}\right)t-\frac{1}{4}\left(\frac{\xi}{\gamma_0}\right)^2\frac{\sin(2\omega_0t)}{2\omega_0}\right]\right\}} \times e^{-i\omega'\sin\theta\cos\Phi\frac{\xi}{\gamma_0\omega_0}\sin(\omega_0t)}dt. \tag{94}$$

If we change the variable to $\tau=\omega_0t$ and expand $\cos\theta$ and $\sin\theta$ as earlier, this can be rewritten as

$$\int_{-\infty}^{\infty}e^{i\omega'(t-\boldsymbol{n}\cdot\boldsymbol{r})}dt=\frac{1}{\omega_0}\int e^{i\omega'\left(\frac{\tau}{2\gamma_0^2\omega_0}\left[1+\frac{1}{2}\xi^2+\gamma_0^2\theta^2\right]\right)} \times e^{i\omega'\left[\frac{1}{8\omega_0}\left(\frac{\xi}{\gamma_0}\right)^2\sin(2\tau)-\theta\cos\Phi\frac{\xi}{\gamma_0\omega_0}\sin(\tau)\right]}d\tau. \tag{95}$$

Now we know that

$$e^{i\omega'\left[\frac{1}{8\omega_0}\left(\frac{\xi}{\gamma_0}\right)^2\sin(2\tau)-\theta\cos\Phi\frac{\xi}{\gamma_0\omega_0}\sin(\tau)\right]} \tag{96}$$

is a 2π periodic function so we can write it as a Fourier series,

$$e^{i\omega'\left[\frac{1}{8\omega_0}\left(\frac{\xi}{\gamma_0}\right)^2\sin(2\tau)-\theta\cos\Phi\frac{\xi}{\gamma_0\omega_0}\sin(\tau)\right]}=\sum_{n=-\infty}^{\infty}A_0(n,\alpha_1,\alpha_2)e^{-in\tau}, \tag{97}$$

where we have defined

$$A_m(n,\alpha_1,\alpha_2)=\frac{1}{2\pi}\int_{-\pi}^{\pi}\cos^m(\tau)e^{i[\alpha_1\sin(\tau)-\alpha_2\sin(2\tau)-n\tau]}d\tau, \tag{98}$$

as in [2,27], with

$$\alpha_1=\theta\cos\Phi\frac{\omega'\xi}{\gamma_0\omega_0}, \tag{99}$$

and

$$\alpha_2=\frac{\omega'}{8\omega_0}\left(\frac{\xi}{\gamma_0}\right)^2. \tag{100}$$

When inserting this in Eq. (95), we obtain

$$\int_{-\infty}^{\infty}e^{i\omega'(t-\boldsymbol{n}\cdot\boldsymbol{r})}dt=\frac{2\pi}{\omega_0}\sum_{n=-\infty}^{\infty}A_0(n,\alpha_1,\alpha_2) \delta\left[\frac{\omega'}{2\gamma_0^2\omega_0}\left(1+\frac{1}{2}\xi^2+\gamma_0^2\theta^2\right)-n\right]. \tag{101}$$

Now calculating $\int_{-\infty}^{\infty}(\boldsymbol{n}-\boldsymbol{v})e^{i\omega'(t-\boldsymbol{n}\cdot\boldsymbol{r})}dt$ is straightforward. For the y component, we have

$$\int_{-\infty}^{\infty}(\boldsymbol{n}-\boldsymbol{v})_ye^{i\omega'(t-\boldsymbol{n}\cdot\boldsymbol{r})}dt=\frac{1}{\omega_0}\int_{-\infty}^{\infty}\left[\theta\cos\Phi-\frac{\xi}{\gamma_0}\cos(\tau)\right] \times e^{i\omega'\left(\frac{\tau}{2\gamma_0^2\omega_0}\left[1+\frac{1}{2}\xi^2+\gamma_0^2\theta^2\right]\right)} \times e^{i\omega'\left[\frac{1}{8\omega_0}\left(\frac{\xi}{\gamma_0}\right)^2\sin(2\tau)-\theta\cos\Phi\frac{\xi}{\gamma_0\omega_0}\sin(\tau)\right]}d\tau. \tag{102}$$

The first term is simply a constant (no τ dependence) times the integral we have already calculated, and the cosine factor in the second term means we simply need to replace $A_0(n,\alpha_1,\alpha_2)$ with $A_1(n,\alpha_1,\alpha_2)$, and so

$$\int_{-\infty}^{\infty}(\boldsymbol{n}-\boldsymbol{v})_ye^{i\omega'(t-\boldsymbol{n}\cdot\boldsymbol{r})}dt =\frac{2\pi}{\omega_0}\sum_{n=-\infty}^{\infty}\left[\theta\cos\Phi A_0(n,\alpha_1,\alpha_2)-\frac{\xi}{\gamma_0}A_1(n,\alpha_1,\alpha_2)\right] \times\delta\left[\frac{\omega'}{2\gamma_0^2\omega_0}\left(1+\frac{1}{2}\xi^2+\gamma_0^2\theta^2\right)-n\right]. \tag{103}$$

The z component is simply a constant times the result from Eq. (101) since $v_z=0$, so we have

$$\int_{-\infty}^{\infty}(\boldsymbol{n}-\boldsymbol{v})_ze^{i\omega'(t-\boldsymbol{n}\cdot\boldsymbol{r})}dt=\frac{2\pi}{\omega_0}\sum_{n=-\infty}^{\infty}\theta\sin\Phi A_0(n,\alpha_1,\alpha_2) \times\delta\left[\frac{\omega'}{2\gamma_0^2\omega_0}\left(1+\frac{1}{2}\xi^2+\gamma_0^2\theta^2\right)-n\right]. \tag{104}$$

In Eq. (93), we see that we need these quantities squared and so we must consider the meaning of the δ function $\delta[\frac{\omega'}{2\gamma_0^2\omega_0}(1+\frac{1}{2}\xi^2+\gamma_0^2\theta^2)-n]$ squared. This came from an integral over

the phase τ and so the usual approach is that

$$\left\{\delta\left[\frac{\omega'}{2\gamma_0^2\omega_0}\left(1+\frac{1}{2}\xi^2+\gamma_0^2\theta^2\right)-n\right]\right\}^2 = \delta\left[\frac{\omega'}{2\gamma_0^2\omega_0}\left(1+\frac{1}{2}\xi^2+\gamma_0^2\theta^2\right)-n\right]\frac{\Delta\tau}{2\pi}, \quad (105)$$

where $\Delta\tau$ is the phase length which is $\omega_0 T$, where T is the interaction time, and which we can divide with on both sides of Eq. (93) to obtain the energy emitted per unit time. We therefore obtain

$$\left|\int (\boldsymbol{n}-\boldsymbol{v})e^{i\omega'(t-\boldsymbol{n}\cdot\boldsymbol{r})}dt\right|^2 = \frac{(2\pi)^2}{\omega_0^2}\frac{T\omega_0}{2\pi}\delta\left[\frac{\omega'}{2\gamma_0^2\omega_0}\left(1+\frac{1}{2}\xi^2+\gamma_0^2\theta^2\right)-n\right] \times\sum_{n=-\infty}^{\infty}\left[\theta\cos\Phi A_0(n,\alpha_1,\alpha_2)-\frac{\xi}{\gamma_0}A_1(n,\alpha_1,\alpha_2)\right]^2 + [\theta\sin\Phi A_0(n,\alpha_1,\alpha_2)]^2. \quad (106)$$

So far we have not considered the contribution from $\int(\boldsymbol{n}-\boldsymbol{v})_x e^{i\omega'(t-\boldsymbol{n}\cdot\boldsymbol{r})}dt$ and this is because it is suppressed compared to the two other terms. As stated by Baier and Katkov, relativistic particles emit radiation predominantly in a cone of angle of the order of $1/\gamma_0$ around their velocity vector, therefore n_y and n_z are of the order of ξ/γ_0 and $1/\gamma_0$, respectively, and therefore we have $n_x - v_x \simeq 1-(n_y^2+n_z^2)/2-(1-1/2\gamma_0^2-\xi^2/4\gamma_0^2)$ where, due to cancellation of the large contributions, we are left with terms only of the order of $1/\gamma_0^2$ or ξ^2/γ_0^2 times the exponential, whereas the y and z terms are of the order of $1/\gamma_0$ or ξ/γ_0 times the same exponential. For this reason, this term can be neglected. Now we wish to carry out the integration over $d\theta$ so, similarly to the reasoning in the context of Eq. (88), we find

$$\delta\left[\frac{\omega'}{2\gamma_0^2\omega_0}\left(1+\frac{1}{2}\xi^2+\gamma_0^2\theta^2\right)-n\right] = \frac{\omega_0}{\omega'\theta}\delta(\theta-\theta_{0,\mathrm{B}}), \quad (107)$$

where

$$\theta_{0,\mathrm{B}} = \frac{1}{\gamma_0}\sqrt{\frac{2\gamma_0^2\omega_0 n}{\omega'}-\left(1+\frac{\xi^2}{2}\right)} = \frac{1}{\gamma_0}\sqrt{\left(1+\frac{\xi^2}{2}\right)\left(\frac{\omega'_{\mathrm{th}}}{\omega'}-1\right)}, \quad (108)$$

where $\omega'_{\mathrm{th}} = 2\gamma_0^2\omega_0 n/(1+\frac{\xi^2}{2})$. We note that while there are obviously two solutions for θ which would make the content of the δ function in Eq. (107) zero, namely, also $-\theta_{0,\mathrm{B}}$, the negative solution is not allowed by our choice of coordinate system where $0\leqslant\theta\leqslant\pi$. Here we see that we should have $n\geqslant 1$ to have any solutions. From this equation, it is clear that for a given quantum number n, the largest allowed value of ω' is ω'_{th} and this is the location of the sharp edges in the spectra seen in Figs. 2–6. It is also seen that most energy is emitted for large ω' within each harmonic peak, and therefore typically $\frac{\omega'_{\mathrm{th}}}{\omega'}-1$ is of the order of 1 and therefore $\theta_{0,\mathrm{B}}$ is typically of the order of ξ/γ_0, and therefore our approximation that $\theta\ll 1$ holds true. Since there are no angular-dependent prefactors in

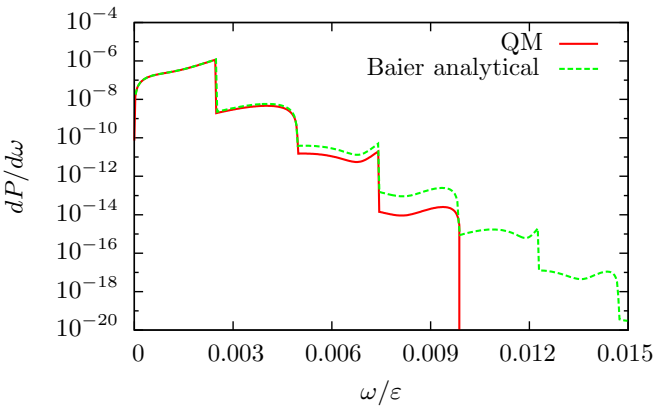

FIG. 2. The case of $n=4$ and $\xi=0.1$. QM: the fully quantum calculation; Baier analytical: the semiclassical method of Baier and Katkov.

Eq. (93), we can carry out the integrals over the angles directly by considering

$$\int d\Phi\theta d\theta\left|\int(\boldsymbol{n}-\boldsymbol{v})e^{i\omega'(t-\boldsymbol{n}\cdot\boldsymbol{r})}dt\right|^2 = \int d\Phi\frac{2\pi T}{\omega'}\sum_{n=-\infty}^{\infty} \times\left[\theta_{0,\mathrm{B}}\cos\Phi A_0(n,\alpha_1,\alpha_2)-\frac{\xi}{\gamma_0}A_1(n,\alpha_1,\alpha_2)\right]^2 + [\theta_{0,\mathrm{B}}\sin\Phi A_0(n,\alpha_1,\alpha_2)]^2, \quad (109)$$

and for the second term of Eq. (93), we obtain

$$\left|\int e^{i\omega'(t-\boldsymbol{n}\cdot\boldsymbol{r})}dt\right|^2 = \frac{2\pi}{\omega_0^2}T\omega_0\sum_{n=-\infty}^{\infty}A_0^2(n,\alpha_1,\alpha_2) \times\delta\left[\frac{\omega'}{2\gamma_0^2\omega_0}\left(1+\frac{1}{2}\xi^2+\gamma_0^2\theta^2\right)-n\right]. \quad (110)$$

Integrating this term over all angles as well, we obtain

$$\int d\Phi\theta d\theta\left|\int e^{i\omega'(t-\boldsymbol{n}\cdot\boldsymbol{r})}dt\right|^2 = \int d\Phi\frac{2\pi T}{\omega'}\sum_{n=-\infty}^{\infty}A_0^2(n,\alpha_1,\alpha_2). \quad (111)$$

So, in total, we obtain the emitted power dP (energy per unit time) differential in the emitted photon energy as

$$\frac{dP}{d\omega} = \frac{e^2}{2\pi}\omega'\int d\Phi\sum_{n=1}^{\infty} \times\left(\frac{\varepsilon'^2+\varepsilon^2}{2\varepsilon^2}\left[\left\{\theta_{0,\mathrm{B}}\cos\Phi A_0(n,\alpha_1,\alpha_2)-\frac{\xi}{\gamma_0}A_1(n,\alpha_1,\alpha_2)\right\}^2 + \{\theta_{0,\mathrm{B}}\sin\Phi A_0(n,\alpha_1,\alpha_2)\}^2\right] + \frac{\omega^2m^2}{2\varepsilon^4}A_0^2(n,\alpha_1,\alpha_2)\right). \quad (112)$$

In this form, it is clear which terms correspond to which from Eq. (93); however, it is not immediately obvious that it is identical to that found in [27]. To ob-

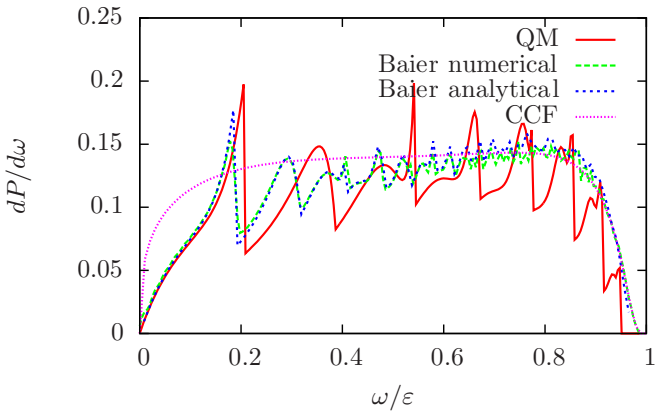

FIG. 3. The case of $n = 8$, $\xi = 5$, $\chi = 7.81$. QM: the fully quantum calculation; Baier numerical: the semiclassical method of Baier and Katkov for 15 periods of oscillation; Baier analytical: the analytical results obtained from the semiclassical method corresponding to the limit of many oscillations; CCF: the constant crossed field approximation. This figure shows the "doubly quantum" regime where the semiclassical method no longer provides accurate results.

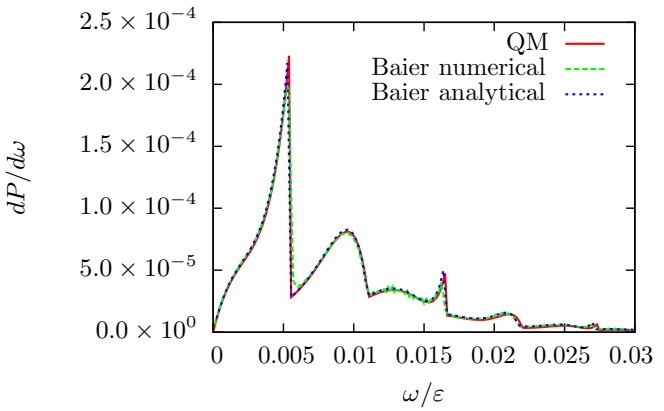

FIG. 4. The case of $n = 120$, $\xi = 1$. QM: the fully quantum calculation; Baier numerical: the semiclassical method of Baier and Katkov for 15 periods of oscillation; Baier analytical: the analytical results obtained from the semiclassical method corresponding to the limit of many oscillations. Here we see how for quite large values of the quantum number, the semiclassical method is good.

tain this, we must carry out the square in the term $\{\theta_{0,\mathrm{B}}\cos\Phi A_0(n,\alpha_1,\alpha_2) - \frac{\xi}{\gamma_0}A_1(n,\alpha_1,\alpha_2)\}^2$. This will give us a term $-2\theta_{0,\mathrm{B}}\cos\Phi A_0(n,\alpha_1,\alpha_2)\frac{\xi}{\gamma_0}A_1(n,\alpha_1,\alpha_2)$, which we will rewrite by employing the relation found in [2] stating that

$$\alpha_1 A_1(n,\alpha_1,\alpha_2) = (n-2\alpha_2)A_0(n,\alpha_1,\alpha_2) + 4\alpha_2 A_2(n,\alpha_1,\alpha_2), \tag{113}$$

and from this we can express $\cos\Phi A_1(n,\alpha_1,\alpha_2)$ in terms of A_0 and A_2, which after some rewriting will lead us to the same result as in [27],

$$\frac{dP}{d\omega} = \frac{e^2}{2\pi}\frac{\omega}{\gamma_0^2}\int d\Phi \sum_{n=1}^{\infty} \times \left\{-A_0^2 + \xi^2\left[1+\frac{u^2}{2(1+u)}\right](A_1^2 - A_0A_2)\right\}, \tag{114}$$

where $u = \frac{\omega}{\varepsilon-\omega}$.

VII. RESULTS AND DISCUSSION

Now we have calculated the radiation emission using two different approaches to the same problem. One is fully quantum mechanical and the other is a semiclassical approach. A third method, which is well known in the literature [69–72], is to approximate the emission as happening in a constant crossed field and use the formula for radiation emission in this case. This is generally considered applicable when $\xi \gg 1$ and so we will also make this comparison when this condition is fulfilled.

When dealing with radiation emission, the quantum parameter is defined by

$$\chi = \frac{e\sqrt{-(F^{\mu\nu}p_\nu)^2}}{m^3}, \tag{115}$$

and tells us how important quantum effects such as recoil and spin are. When $\chi \ll 1$, these effects are small. However the effect of low quantum number is not covered by this parameter and is a separate condition. We will consider the peak field value in terms of the parameters of our problem, which is then given by

$$\chi_{\max} = \kappa y_{\max}\frac{2\gamma_0}{E_c}. \tag{116}$$

From the discussion below Eq. (60), we have that $y_{\max}$ can also be accurately written as $y_{\max} = L\sqrt{2n}$ when n is large, so

$$\chi_{\max} = \kappa\sqrt{2n}L\frac{2\gamma_0}{E_c}. \tag{117}$$

Setting $p_x \simeq \varepsilon$ and $\beta_{\mathrm{b}} \simeq 1$, we have

$$\frac{1}{L} \simeq \sqrt[4]{2e\kappa p_x}, \tag{118}$$

$$\frac{1}{2p_x L^4} = e\kappa, \tag{119}$$

and so we have

$$\chi_{\max} = \sqrt{2n}\left(\frac{\lambda_C}{L}\right)^3, \tag{120}$$

where $\lambda_C = 1/m$ is the Compton wavelength. In the special case of the harmonic oscillator, the momentum-space wave function is the same as the space wave function save only for a different variable, such that instead of $I_n(y/L)$, we have $I_n(q_y L)$, and therefore since the function $I_n(\eta)$ decreases rapidly for $\eta^2 > 2n$, we can also write $q^2_{y,\max} = 2n/L^2$. And so we express the other parameter usually considered when dealing with radiation emission ξ in terms of the parameters of our solutions to obtain

$$\xi = \frac{q_{y,\max}}{m} = \frac{\lambda_C}{L}\sqrt{2n}. \tag{121}$$

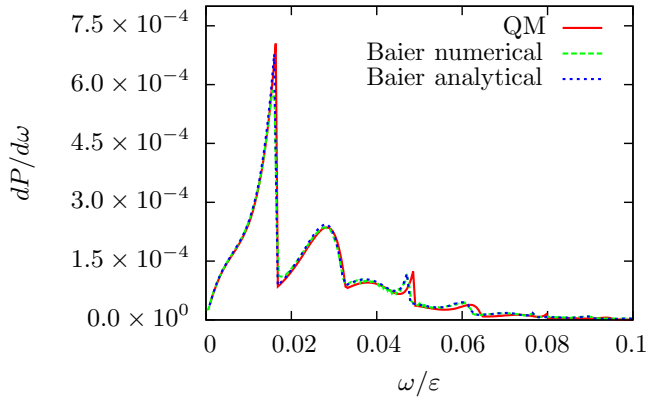

FIG. 5. The case of $n = 40$, $\xi = 1$. QM: the fully quantum calculation; Baier numerical: the semiclassical method of Baier and Katkov for 15 periods of oscillation; Baier analytical: the analytical results obtained from the semiclassical method corresponding to the limit of many oscillations. Here we see how for smaller values of the quantum number, one begins to see small deviations between the semiclassical method and the correct result.

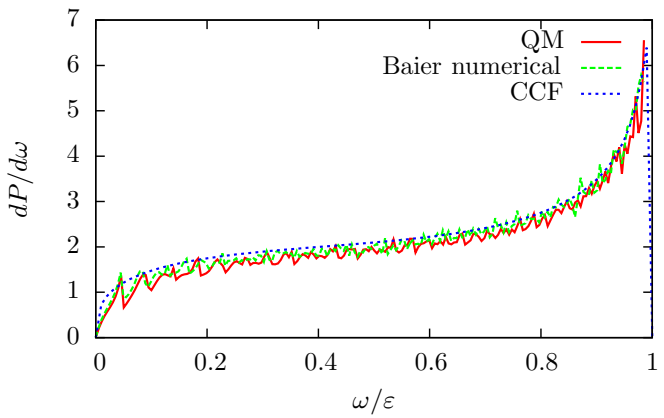

FIG. 6. The case of $n = 40$, $\xi = 30$. QM: the fully quantum calculation; Baier numerical: the semiclassical method of Baier and Katkov for 15 periods of oscillation; CCF: the constant crossed field approximation. Here we see how, also in the regime where the CCF approximation may be applied, the deviation from the correct results is small when $n = 40$.

And, combining this with Eq. (120), we obtain the useful relation

$$\chi_{\max} = \frac{\xi^3}{2n}. \tag{122}$$

For weak fields, meaning a small field gradient κ, L will become large and so we will denote $L \gg \lambda_C$ as the weak-field gradient regime, and vice versa. Below we will discuss features of the radiation spectrum shown in the figures in the different regimes. In the figures, QM corresponds to the exact calculation of Eq. (91) and Baier analytical corresponds to Eq. (114). Baier numerical corresponds to using the formula of Eq. (93) by numerically solving the equations of motion corresponding to a time of 15 oscillations in the field numerically, and then performing the integration over angles and time numerically, as done in [47]. CCF corresponds to the radiation emitted when applying the constant crossed field approximation.

A. Weak-field gradient regime, $L \gg \lambda_C$

In this regime when the quantum number n is small, both $\chi_{\max}$ and ξ will be small as seen from Eqs. (120) and (121). A small value of $\chi_{\max}$ means the only quantum effects for n small are those due to the quantization of the motion. Since ξ will be small, the radiation is in the dipole regime, meaning different harmonics are clear and most radiation comes from the first harmonic. In Fig. 2, we have shown a plot of the radiation spectrum in this regime using the exact calculation and the semiclassical approximation. Coincidentally, the two calculations yield the same result for the first harmonic, and differences are only seen for higher harmonics. So differences are only seen in the parts of the spectrum where the radiation yield is small. Another difference is that the exact calculation only allows a finite number of harmonics corresponding to transitions from the initial state with quantum number n_i to one with lower quantum number, and the last harmonic thus corresponds to transition to the ground state and, for photon energies above the threshold corresponding to this harmonic, no radiation can be emitted. With the semiclassical method, this is not the case and the sum over harmonics is infinite.

B. Strong-field gradient regime, $L \ll \lambda_C$

If one wants to see big differences in the whole of the spectrum, as seen in Fig. 3, one must be in the strong-field regime and have small value of n. In this regime, one will always have large χ such that recoil and spin is important, and for small n, one has the additional quantum effect of the quantized motion, i.e., one needs the wave function instead of the trajectory.

In Fig. 3, we have shown an example of this which could be dubbed the "doubly quantum regime," where it is seen that the correct calculation deviates significantly from the constant crossed field approximation (CCF), but also from the result of the semiclassical operator method which is more general, and evidently fails in the regime of low quantum numbers. This transition from the usual regime to the doubly quantum regime happens when the n quantum number is small and $L = \frac{1}{m}$, which can be related to a certain beam density as we will see in Sec. VII D.

In Figs. 4 and 5, the radiation spectrum for $\xi = 1$, but for a different value of the quantum number n of the radiating particles. Here it is seen that as n is large, as in the $n = 120$ case, the agreement between the exact calculation and the semiclassical approach is good, while when it becomes smaller, in the case of $n = 40$, the agreement becomes worse. In Fig. 6, we show the radiation spectrum in the regime where the constant crossed field approximation is applicable and see that while there are small differences between the semiclassical method and the exact calculation in the position of the harmonics (see, e.g., the position of the third and fourth harmonic peaks), the overall size of the spectrum coincides quite well, while the CCF approximation seems to slightly overestimate the radiation emitted at low frequencies. So to see major differences, one needs an even smaller value of n, as is the case seen in Fig. 3.

C. Effects for planar channeling of positrons

Channeling is the phenomenon of high-energy particles being transversely trapped between planes or between strings in a crystal [27,73,74]. In the particular case of positrons trapped between crystal planes, the potential governing their motion is quite close to that of the parabolic potential, which we have treated in this paper. Therefore, it is natural to ask if the results we find would apply to the case of channeling. In this case, the largest allowed value of y is $d_p/2$, where d_p is the distance between two planes. Here we can write the potential energy as $U(y) = 4U_0 y^2/d_p^2$, where U_0 is the potential-energy depth. The parameters U_0 and d_p can be looked up in, e.g., [27]. Based on this way of writing the potential energy, we have that $\kappa = 8U_0/ed_p^2$ and, inserting this in Eq. (57) and then using $y_{\max} = L\sqrt{2n_{\max}}$, one obtains $n_{\max} = (d_p/2)(\sqrt{U_0 m/2})\sqrt{\gamma_0}$. The factor $(d_p/2)(\sqrt{U_0 m/2})$ is of the order of 1 and therefore we have roughly $n_{\max} \simeq \sqrt{\gamma_0}$. Therefore, we see that in order to have a small quantum number, we also need quite low particle energy, i.e., $n_{\max} = 10$ corresponds to an energy of roughly 50 MeV. The weak-field gradient regime $L \gg \lambda_C$ then corresponds to $\varepsilon \ll \varepsilon_c$, where $\varepsilon_c = m^4 d_p^2/8U_0$. For the most optimistic case, we can insert the values for tungsten and obtain $\varepsilon_c = 21.2$ TeV, and therefore the condition of low quantum number also means we will be in the weak-field gradient regime. In this regime, the spectrum would be similar to the one seen in Fig. 2. For channeling, one has the critical angle given by $\theta_c = \sqrt{2U_0/\varepsilon}$ and therefore we have $\xi = \sqrt{2U_0/m}\sqrt{\gamma_0} \simeq n_{\max}\sqrt{2U_0/m}$, and therefore we see that if we want a small quantum number, we will also be in the dipole regime. For this reason, in [27], there is a section on calculating the (dominant) radiation from the first harmonic in this regime of low quantum numbers which does not use their developed semiclassical method; however, the higher harmonics, where one would start to see a deviation, are not treated.

D. Effects for beamstrahlung

To gain an understanding of when these effects could arise in beamstrahlung, we wish to approximate the parameters we have introduced in terms of the usually given beam parameters; see Table I. From Eq. (9), we have that κ relates to the peak density as

$$\kappa = 4\pi\rho_0, \tag{123}$$

where $\rho_0 = \rho(\vec{0})$. So, using Eq. (119), we have

$$\frac{1}{L^4} = 8\pi e\rho_0\varepsilon. \tag{124}$$

Now we can define the critical density ρ_c as that corresponding to $L = 1/m$ so $m^4 = 8\pi e\rho_c\varepsilon$, or

$$\rho_c = \frac{m^4}{8\pi e\varepsilon}. \tag{125}$$

So, to be in the doubly quantum regime, one should reach this density and have a small quantum number, i.e., where the transverse beam size becomes comparable to the Compton wavelength. This also gives us another way of expressing the length parameter of the problem L in terms of the critical density since

$$\frac{1}{L^4} = m^4\frac{\rho_0}{\rho_c}, \tag{126}$$

and so we also have

$$\left(\frac{\lambda_C}{L}\right)^4 = \frac{\rho_0}{\rho_c}. \tag{127}$$

Now we can use Eq. (120) to obtain an estimate of the quantum number corresponding to the particles with the largest amplitude, which will contribute most to the radiation spectrum. This gives us

$$\sqrt{2n_{\max}} = \chi_{\max}/\left(\frac{\rho_0}{\rho_c}\right)^{3/4}. \tag{128}$$

Now we wish to obtain an expression giving us the quantum number corresponding to the largest amplitude of oscillation when crossing a bunch in terms of the usual beam parameters such that we can see how this scales and in what regime these effects would become important. We have

$$\frac{\rho_0}{\rho_c} = \frac{Ne}{(2\pi)^{3/2}\Sigma_x\Sigma_y\Sigma_z}\frac{8\pi e\varepsilon}{m^4} = \frac{8\pi Ne^2\gamma_0}{(2\pi)^{3/2}\Sigma_x\Sigma_y\Sigma_z m^3}. \tag{129}$$

TABLE I. Beam parameters.

Machine	CLIC	CLIC	ILC	ILC	HER 2017	CLIC mod.
ε	190 GeV	1500 GeV	100 GeV	250 GeV	4 GeV	1500 GeV
N	5.2×10^9	3.7×10^9	2.0×10^{10}	2.0×10^{10}	6.5×10^{10}	3.7×10^9
Σ_x	149 nm	40 nm	904 nm	474 nm	10.7 μm	4 μm
Σ_y	2.9 nm	1 nm	7.8 nm	5.9 nm	62 nm	10 pm
Σ_z	70 μm	44 μm	300 μm	300 μm	5 mm	44 μm
$\chi_{\max}$	0.32	10.7	0.025	0.12	1.65×10^{-5}	0.11
$\rho_{\max}$	7.13×10^6 eV^3	8.72×10^7 eV^3	3.92×10^5 eV^3	9.89×10^5 eV^3	8.16×10^2 eV^3	8.72×10^7 eV^3
ρ_c	1.67×10^{11} eV^3	2.12×10^{10} eV^3	3.18×10^{11} eV^3	1.27×10^{11} eV^3	7.9×10^{12} eV^3	2.12×10^{10} eV^3
λ_C/L	0.081	0.25	0.033	0.0528	0.0032	0.25
$\sqrt{2n_{\max}}$	608	657	674	808	512	6.6
$\xi_{\max}$	49	166	22.5	43	1.63	1.67

Now we use Eq. (116) and insert κ from Eq. (9) and, to obtain an estimate for the typical beam particle, we set $y_{\max} = \Sigma_y$,

$$\chi_{\max} = \frac{4\gamma_0 N e^2}{\sqrt{2\pi} m^2 \Sigma_x \Sigma_z}.$$

So, introducing $o_i = \Sigma_i m$, we have

$$\begin{aligned}\chi_{\max}/\left(\frac{\rho_0}{\rho_c}\right)^{3/4} &= \frac{4\gamma_0 N e^2}{\sqrt{2\pi} o_x o_z}\left(\frac{(2\pi)^{3/2} o_x o_y o_z}{8\pi N e^2 \gamma_0}\right)^{3/4} \\ &= \sqrt[4]{\frac{4}{\sqrt{2\pi}}}\frac{(o_x o_y o_z)^{3/4}}{o_x o_z}(N\gamma_0 e^2)^{1/4},\end{aligned} \tag{130}$$

and so

$$n_{\max} = \frac{1}{\sqrt[4]{2\pi}}\frac{(o_x o_y o_z)^{3/2}}{(o_x o_z)^2}(N\gamma_0 e^2)^{1/2}. \tag{131}$$

To obtain an expression for ξ, we can use the expression for the amplitude given by Eq. (26) and set it equal to Σ_y so that

$$\xi_{\max} = \Sigma_y \gamma_0 \sqrt{\frac{2e\kappa}{\varepsilon}} = \frac{2}{(2\pi)^{1/4}}\sqrt{\frac{N e^2 \gamma_0 o_y}{o_x o_z}}. \tag{132}$$

From the facts that $y_{\max} = L\sqrt{2n}$ and the transition to the doubly quantum regime happens when $L \simeq 1/m$ and n small, we can get an estimate of how small the beam size has to be. So, we have $\Sigma_{y,\mathrm{crit}} \simeq 10\lambda_C\sqrt{20} = 17$ pm. Currently, the accelerator SuperKEKB has beams with a size of 62 nm, while future machines such as Compact Linear Collider (CLIC) has proposed 1 nm beams. In Table I, we have shown the beam parameters of a current electron-positron accelerator, superKEKB, along with some that are still on the drawing board, namely, the CLIC and International Linear Collider (ILC). From the large value of $\sqrt{2n_{\max}}$, it is clear that the effects we have seen in this paper will not be important, i.e., the semiclassical method will provide the correct result. If the beams are reshaped, making them even smaller in the y direction and larger in the x direction, $n_{\max}$ will go down, as can be seen from Eq. (131). For the High-Energy Ring (HER) (SuperKEKB), if we reduce Σ_y by a factor of 100 and increase Σ_x by the same amount, the luminosity is unchanged but we then have $n_{\max} = 13$. However, because of the low energy and so, not being close to the critical density ρ_c, we would only be in the weak-field gradient regime where $\chi_{\max} \ll 1$. To be in the doubly quantum regime, we have considered CLIC with 3 TeV center-of-mass energy and reshaped the beams in the same way. This is the "CLIC mod." case from Table I. Here it is seen that $\chi_{\max} = 0.11$, so the usual quantum effects would start to come into play and, at the same time, we have a small quantum number of $n_{\max} = 22$. We point out that simply reshaping the beams with a focusing magnet is not sufficient to reach the regime where all particles would radiate in this regime. For this we would also require that the distribution of angles of the particles in the y direction remains smaller than the typical oscillation angle ξ/γ_0. These two conditions together, where the beam should be small and the angles should also be under a certain limit, can be summarized by a requirement on the beam emittance, namely,

$$\gamma_0 \epsilon_y \lesssim 2n\lambda_C, \tag{133}$$

where ϵ_y is the emittance in the y direction and, therefore, the left-hand side is the normalized emittance. This reshaping of the beams would be beneficial since χ is reduced while keeping the luminosity the same, thus reducing the emitted energy to beamstrahlung. This is the original purpose of having the bunches shaped like sheets. We see here that if this strategy is taken to the extreme, one will enter this regime of radiation emission, where the quantization of the transverse motion becomes important.

VIII. CONCLUSION

From first principles, we have found approximate wave functions for a relativistic spin-$\frac{1}{2}$ particle in a harmonic-oscillator-like potential, valid when $\xi/\gamma_0 \ll 1$ and $\gamma_0 \gg 1$, and calculated the radiation emission spectrum which showed interesting features, allowing us to find a regime of radiation emission where another quantum effect besides the usual ones comes into play, namely, the quantization of the motion. This effect is absent in the well-studied examples of nonlinear Compton scattering in a plane wave where the semiclassical method of Baier and Katkov yields the correct result. On the contrary, in the field configuration studied here, there is, in fact, a difference between the two methods and the semiclassical operator method fails for low quantum numbers. This means that the results obtained here could not have been obtained in the simpler way of using the semiclassical method. Therefore, these findings are interesting in their own right. We found that for low quantum numbers, there will always be a difference between the two calculations; however, in the weak-field gradient regime, the differences will only be for the higher harmonics where the spectral yield is already low. Only in the strong-field gradient regime, where quantum effects such as spin and recoil also come into play, can one have large deviations between the two calculations. We applied our calculation as a model to two radiation emission phenomena, i.e., planar channeling of positrons and the case of beamstrahlung, to see when one would enter the regime of low transverse quantum number. For channeling, we found that we would be in the weak-field gradient regime. For beamstrahlung, we found that current machines and the ones currently on the drawing board are far from being in the regime of low quantum numbers; however, if the strategy of making bunches shaped like sheets, which is the strategy to avoid energy loss due to beamstrahlung, is taken to the extreme, one enters this regime of radiation emission where the quantization of the motion of the radiating particle becomes important.

ACKNOWLEDGMENT

For this research project T.N.W. was supported by the research grant (Grant No. VKR023371) from VILLUM FONDEN.

[1] H. Mitter, in *Quantum Electrodynamics in Laser Fields, Electromagnetic Interactions and Field Theory*, edited by P. Urban (Springer, Vienna, 1975), pp. 397–468.

[2] V. I. Ritus, Quantum effects of the interaction of elementary particles with an intense electromagnetic field, J. Sov. Laser Res. **6**, 497 (1985).

[3] F. Ehlotzky, K. Krajewska, and J. Z. Kamiński, Fundamental processes of quantum electrodynamics in laser fields of relativistic power, Rep. Progr. Phys. **72**, 046401 (2009).

[4] A. Di Piazza, C. Müller, K. Z. Hatsagortsyan, and C. H. Keitel, Extremely high-intensity laser interactions with fundamental quantum systems, Rev. Mod. Phys. **84**, 1177 (2012).

[5] S. P. Roshchupkin, A. A. Lebed', E. A. Padusenko, and A. I. Voroshilo, Quantum electrodynamics resonances in a pulsed laser field, Laser Phys. **22**, 1113 (2012).

[6] F. Karbstein, H. Gies, M. Reuter, and M. Zepf, Vacuum birefringence in strong inhomogeneous electromagnetic fields, Phys. Rev. D **92**, 071301 (2015).

[7] J. J. Klein and B. P. Nigam, Birefringence of the vacuum, Phys. Rev. **135**, B1279 (1964).

[8] V. Dinu, T. Heinzl, A. Ilderton, M. Marklund, and G. Torgrimsson, Vacuum refractive indices and helicity flip in strong-field QED, Phys. Rev. D **89**, 125003 (2014).

[9] T. Heinzl, B. Liesfeld, K.-U. Amthor, H. Schwoerer, R. Sauerbrey, and A. Wipf, On the observation of vacuum birefringence, Opt. Commun. **267**, 318 (2006).

[10] S. L. Adler, Vacuum birefringence in a rotating magnetic field, J. Phys. A: Math. Theor. **40**, F143 (2007).

[11] T. N. Wistisen and U. I. Uggerhøj, Vacuum birefringence by Compton backscattering through a strong field, Phys. Rev. D **88**, 053009 (2013).

[12] S. Bragin, S. Meuren, C. H. Keitel, and A. Di Piazza, High-Energy Vacuum Birefringence and Dichroism in an Ultrastrong Laser Field, Phys. Rev. Lett. **119**, 250403 (2017).

[13] N. B. Narozhny and M. S. Fofanov, Quantum processes in a two-mode laser field, J. Exp. Theor. Phys. **90**, 415 (2000).

[14] S. P. Roshchupkin, Interference effect in the photoproduction of electron-positron pairs on a nucleus in the field of two light waves, Phys. At. Nucl. **64**, 243 (2001).

[15] T. Heinzl, A. Ilderton, and M. Marklund, Finite size effects in stimulated laser pair production, Phys. Lett. B **692**, 250 (2010).

[16] T.-O. Müller and C. Müller, Spin correlations in nonperturbative electron–positron pair creation by petawatt laser pulses colliding with a TeV proton beam, Phys. Lett. B **696**, 201 (2011).

[17] A. I. Titov, H. Takabe, B. Kämpfer, and A. Hosaka, Enhanced Subthreshold e^+e^- Production in Short Laser Pulses, Phys. Rev. Lett. **108**, 240406 (2012).

[18] T. Nousch, D. Seipt, B. Kämpfer, and A. I. Titov, Pair production in short laser pulses near threshold, Phys. Lett. B **715**, 246 (2012).

[19] K. Krajewska, C. Müller, and J. Z. Kamiński, Bethe-Heitler pair production in ultrastrong short laser pulses, Phys. Rev. A **87**, 062107 (2013).

[20] M. J. A. Jansen and C. Müller, Strongly enhanced pair production in combined high- and low-frequency laser fields, Phys. Rev. A **88**, 052125 (2013).

[21] S. Augustin and C. Müller, Nonperturbative Bethe–Heitler pair creation in combined high- and low-frequency laser fields, Phys. Lett. B **737**, 114 (2014).

[22] A. Di Piazza, K. Z. Hatsagortsyan, and C. H. Keitel, Nonperturbative Vacuum-Polarization Effects in Proton-Laser Collisions, Phys. Rev. Lett. **100**, 010403 (2008).

[23] S. Meuren and A. Di Piazza, Quantum Electron Self-Interaction in a Strong Laser Field, Phys. Rev. Lett. **107**, 260401 (2011).

[24] A. Di Piazza, On refractive processes in strong laser field quantum electrodynamics, Ann. Phys. (NY) **338**, 302 (2013).

[25] V. Dinu, T. Heinzl, A. Ilderton, M. Marklund, and G. Torgrimsson, Photon polarization in light-by-light scattering: Finite size effects, Phys. Rev. D **90**, 045025 (2014).

[26] H. Gies, F. Karbstein, and R. Shaisultanov, Laser photon merging in an electromagnetic field inhomogeneity, Phys. Rev. D **90**, 033007 (2014).

[27] V. N. Baier, V. M. Katkov, and V. M. Strakhovenko, *Electromagnetic Processes at High Energies in Oriented Single Crystals* (World Scientific, Singapore, 1998).

[28] F. Mackenroth and A. Di Piazza, Nonlinear Double Compton Scattering in the Ultrarelativistic Quantum Regime, Phys. Rev. Lett. **110**, 070402 (2013).

[29] A. Di Piazza, M. Tamburini, S. Meuren, and C. H. Keitel, Implementing nonlinear Compton scattering beyond the local constant field approximation, Phys. Rev. A **98**, 012134 (2018).

[30] V. Yu. Kharin, D. Seipt, and S. G. Rykovanov, Higher-Dimensional Caustics in Nonlinear Compton Scattering, Phys. Rev. Lett. **120**, 044802 (2018).

[31] M. Fuchs, M. Trigo, J. Chen, S. Ghimire, S. Shwartz, M. Kozina, M. Jiang, T. Henighan, C. Bray, G. Ndabashimiye *et al.*, Anomalous nonlinear X-ray Compton scattering, Nat. Phys. **11**, 964 (2015).

[32] T. N. Wistisen, Quantum synchrotron radiation in the case of a field with finite extension, Phys. Rev. D **92**, 045045 (2015).

[33] E. Raicher, S. Eliezer, and A. Zigler, A novel solution to the Klein–Gordon equation in the presence of a strong rotating electric field, Phys. Lett. B **750**, 76 (2015).

[34] K. K. Andersen, J. Esberg, H. Knudsen, H. D. Thomsen, U. I. Uggerhøj, P. Sona, A. Mangiarotti, T. J. Ketel, A. Dizdar, and S. Ballestrero, Experimental investigations of synchrotron radiation at the onset of the quantum regime, Phys. Rev. D **86**, 072001 (2012).

[35] C. Bula, K. T. McDonald, E. J. Prebys, C. Bamber, S. Boege, T. Kotseroglou, A. C. Melissinos, D. D. Meyerhofer, W. Ragg, D. L. Burke, R. C. Field, G. Horton-Smith, A. C. Odian, J. E. Spencer, D. Walz, S. C. Berridge, W. M. Bugg, K. Shmakov, and A. W. Weidemann, Observation of Nonlinear Effects in Compton Scattering, Phys. Rev. Lett. **76**, 3116 (1996).

[36] M. Boca and V. Florescu, Nonlinear Compton scattering with a laser pulse, Phys. Rev. A **80**, 053403 (2009).

[37] C. Harvey, T. Heinzl, and A. Ilderton, Signatures of high-intensity Compton scattering, Phys. Rev. A **79**, 063407 (2009).

[38] T. Heinzl and A. Ilderton, A Lorentz and gauge invariant measure of laser intensity, Opt. Commun. **282**, 1879 (2009).

[39] F. Mackenroth, A. Di Piazza, and C. H. Keitel, Determining the Carrier-Envelope Phase of Intense Few-Cycle Laser Pulses, Phys. Rev. Lett. **105**, 063903 (2010).

[40] F. Mackenroth and A. Di Piazza, Nonlinear Compton scattering in ultrashort laser pulses, Phys. Rev. A **83**, 032106 (2011).

[41] D. Seipt and B. Kämpfer, Nonlinear Compton scattering of ultrashort intense laser pulses, Phys. Rev. A **83**, 022101 (2011).

[42] K. Krajewska and J. Z. Kamiński, Compton process in intense short laser pulses, Phys. Rev. A **85**, 062102 (2012).
[43] D. Seipt and B. Kämpfer, Asymmetries of azimuthal photon distributions in nonlinear Compton scattering in ultrashort intense laser pulses, Phys. Rev. A **88**, 012127 (2013).
[44] V. Dinu, Exact final-state integrals for strong-field QED Phys. Rev. A **87**, 052101 (2013).
[45] V. N. Nedoreshta, A. I. Voroshilo, and S. P. Roshchupkin, Resonant scattering of a photon by an electron in the moderately-strong-pulsed laser field, Phys. Rev. A **88**, 052109 (2013).
[46] K. Krajewska, M. Twardy, and J. Z. Kamiński, Supercontinuum and ultrashort-pulse generation from nonlinear Thomson and Compton scattering, Phys. Rev. A **89**, 032125 (2014).
[47] T. N. Wistisen, Interference effect in nonlinear Compton scattering, Phys. Rev. D **90**, 125008 (2014).
[48] A. Angioi, F. Mackenroth, and A. Di Piazza, Nonlinear single Compton scattering of an electron wave packet, Phys. Rev. A **93**, 052102 (2016).
[49] A. Di Piazza, First-order strong-field QED processes in a tightly focused laser beam, Phys. Rev. A **95**, 032121 (2017).
[50] B. King, Double Compton scattering in a constant crossed field, Phys. Rev. A **91**, 033415 (2015).
[51] A. Di Piazza, Ultrarelativistic Electron States in a General Background Electromagnetic Field, Phys. Rev. Lett. **113**, 040402 (2014).
[52] A. Di Piazza, Analytical tools for investigating strong-field QED processes in tightly focused laser fields, Phys. Rev. A **91**, 042118 (2015).
[53] A. Di Piazza, Nonlinear Breit-Wheeler Pair Production in a Tightly Focused Laser Beam, Phys. Rev. Lett. **117**, 213201 (2016).
[54] T. Heinzl, A. Ilderton, and B. King, Classical and quantum particle dynamics in univariate background fields, Phys. Rev. D **94**, 065039 (2016).
[55] T. Heinzl and A. Ilderton, Exact Classical and Quantum Dynamics in Background Electromagnetic Fields, Phys. Rev. Lett. **118**, 113202 (2017).
[56] T. Heinzl and A. Ilderton, Superintegrble relativistic systems in spacetime-dependent background fields, J. Phys. A: Math. Theor. **50**, 345204 (2017).
[57] V. N. Baier and V. M. Katkov, Processes involved in the motion of high energy particles in a magnetic field, Sov. Phys. JETP **26**, 854 (1968).
[58] D. Itô, K. Mori, and E. Carriere, An example of dynamical systems with linear trajectory, Il Nuovo Cimento A **51**, 1119 (1967).
[59] M. Moshinsky and A. Szczepaniak, The Dirac oscillator, J. Phys. A: Math. Gen. **22**, L817 (1989).
[60] M. Moreno and A. Zentella, Covariance, CPT and the Foldy-Wouthuysen transformation for the Dirac oscillator, J. Phys. A: Math. Gen. **22**, L821 (1989).
[61] J. Bentez, R. P. Martnez y Romero, H. N. Núez-Yépez, and A. L. Salas-Brito, Solution and Hidden Supersymmetry of a Dirac Oscillator, Phys. Rev. Lett. **64**, 1643 (1990).
[62] P. Strange, *Relativistic Quantum Mechanics: With Applications in Condensed Matter and Atomic Physics* (Cambridge University Press, Cambridge, 1998).
[63] R. Wanzenberg, Nonlinear motion of a point charge in the 3D space charge field of a Gaussian bunch, Tech. Rep. No. DESY M 10-01, Deutsches Elektronen-Synchrotron (DESY, Hamburg, Germany, 2010).
[64] K. Takayama, Potential of a three-dimensional charge distribution powerful calculating method and its applications, Tech. Rep. No. TM-1092, Fermi National Accelerator Laboratory (FNAL, Batavia, IL, 1982).
[65] V. B. Beresteckij, E. M. Lifsic, and L. P. Pitaevskij, *Quantum Electrodynamics* (Butterworth-Heinemann, Oxford, 2008).
[66] V. G. Bagrov and D. Gitman, *Exact Solutions of Relativistic Wave Equations* (Springer Science & Business Media, New York, 1990), Vol. 39.
[67] D. J. Griffiths, *Introduction to Quantum Mechanics* (Cambridge University Press, Cambridge, 2016).
[68] A. Belkacem, N. Cue, and J. C. Kimball, Theory of crystal-assisted radiation and pair creation for imperfect alignment, Phys. Lett. A **111**, 86 (1985).
[69] N. Neitz and A. Di Piazza, Stochasticity Effects in Quantum Radiation Reaction, Phys. Rev. Lett. **111**, 054802 (2013).
[70] T. G. Blackburn, C. P. Ridgers, J. G. Kirk, and A. R. Bell, Quantum Radiation Reaction in Laser–Electron-Beam Collisions, Phys. Rev. Lett. **112**, 015001 (2014).
[71] A. Di Piazza, K. Z. Hatsagortsyan, and C. H. Keitel, Quantum Radiation Reaction Effects in Multiphoton Compton Scattering, Phys. Rev. Lett. **105**, 220403 (2010).
[72] T. N. Wistisen, A. Di Piazza, H. V. Knudsen, and U. I. Uggerhøj, Experimental evidence of quantum radiation reaction in aligned crystals, Nat. Commun. **9**, 795 (2018).
[73] J. Lindhard, Influence of crystal lattice on motion of energetic charged particles, Kgl. Dan. Vidensk. Selsk., Mat.-Fys. Medd. **34**, 64 (1965).
[74] U. I. Uggerhøj, The interaction of relativistic particles with strong crystalline fields, Rev. Mod. Phys. **77**, 1131 (2005).